Ion exchange equilibrium and structural changes in clinoptilolite irradiated with - and -radiation: Monovalent cations

ARTICLE *in* AMERICAN MINERALOGIST · OCTOBER 2007

Impact Factor: 1.96 · DOI: 10.2138/am.2007.2545

3 AUTHORS:

Daniel Moraetis
Sultan Qaboos University
31 PUBLICATIONS **119** CITATIONS
SEE PROFILE

G.E. Christidis
Technical University of Crete
48 PUBLICATIONS **690** CITATIONS
SEE PROFILE

Vassilis Perdikatsis
Technical University of Crete
78 PUBLICATIONS **490** CITATIONS
SEE PROFILE

American Mineralogist, Volume 92, pages 1714–1730, 2007

Ion exchange equilibrium and structural changes in clinoptilolite irradiated with β- and γ-radiation: Monovalent cations

Daniel Moraetis,* George E. Christidis, and Vasilios Perdikatsis

Department of Mineral Resources Engineering, Technical University of Crete, 73100, Chania, Greece

Abstract

Thermodynamic calculations of ion-exchange reactions were applied for clinoptilolite in a natural state and after irradiation with three doses of β-radiation (10^{12}, 10^{15}, 3×10^{16} e/cm^2) and γ-radiation (70 Mrad). Samples were equilibrated with binary systems of $K^+ \leftrightarrow Na^+$ and $Cs^+ \leftrightarrow Na^+$ at 25° and a total normality of 0.025 *N*. Selectivity for K was not affected after β-radiation with doses of 10^{12} and 10^{15} e/cm^2 ($\Delta G° = -6.37$ kJ/equiv, $\ln K\alpha = 2.58$ for the original clinoptilolite), whereas it increased considerably after 70 Mrad of γ-radiation ($\Delta G° = -7.88$ kJ/equiv, $\ln K\alpha = 3.18$). Selectivity for Cs^+ increased for the clinoptilolite irradiated with β-radiation (10^{12}, 10^{15}, 3×10^{16} e/cm^2) and γ-radiation (70 Mrad). $\Delta G°$ and $\ln K\alpha$ for original sample and $Cs^+ \leftrightarrow Na^+$ were –7.33 kJ/equiv and 2.96, respectively. Irradiated samples with β-radiation 10^{12}, 10^{15}, 3×10^{16} e/cm^2 and 70 Mrad γ-radiation yielded $\Delta G°$ and $\ln K\alpha$ –7.41, –8.83, –8.60, –8.25 kJ/equiv and 2.99, 3.57, 3.47, 3.33 for $Cs^+ \leftrightarrow Na^+$, respectively. Remarkable amorphization of clinoptilolite was observed after exposure at the highest dose of β-radiation (3×10^{16} e/cm^2) with a concomitant decrease in cation-exchange capacity (CEC). Crystallographic parameters and especially exchangeable cation site coordinates were refined for all samples with the Rietveld method. Cesium-saturated samples exhibited changes in the cation sites Cs2 and Cs3, which are next to clinoptilolite channel walls with lower Al^{3+} for Si^{4+} substitution. The observed changes include a shift in cation sites Cs2 and Cs3 toward channel walls and occupancy decrease in site Cs2.

Keywords: Clinoptilolite, ion exchange, β-radiation, γ-radiation, thermodynamics, Rietveld refinement

Introduction

Clinoptilolite, a HEU-type zeolite, occurs in various geological environments and forms mainly by alteration of volcanic glass, biogenic silica, and clay minerals (Hay 1977; Gottardi 1989; Hay and Sheppard 2001). The ion exchange properties of clinoptilolite have been thoroughly studied in the past by numerous researchers (Ames 1960; Loizidou 1982; Loizidou and Townsend 1987; Pabalan 1994, among others). The ion-exchange properties of zeolites are utilized in environmental applications such as the removal of NH_4^+ from municipal wastewater, the removal of heavy metals mainly from industrial processes (Zamzow et al. 1990; Inglezakis et al. 2004; Petrus and Warchol et al. 2005; Melamed and Benvindo da Luz 2006), or other processes such as the removal and recovery of *p*-phenylenediamines developing compounds from photofinishing lab-wastewater (Vlessidis et al. 2001). In addition, the nuclear industry has invested time and financial resources to solve the problem of nuclear wastewater treatment (treatment of low- and high-level effluents). In the past, several workers have demonstrated the ion-exchange selectivity of clinoptilolite for the removal of radioactive elements like ^{137}Cs from aqueous solutions (Mercer and Ames 1978; Faghihian et al. 1999; Elizondo et al. 2000; Abusafa and Yücel 2002). A more practical application for nuclear wastewater treatment is the Yucca Mountain project in Nevada, U.S.A., which is being investigated as a site for a high-level waste geologic repository. In this example, zeolitized tuffs could act as naturally occurring barriers against radionuclide transport (Bodvarsson et al. 1999; Vaniman et al. 2001). In the case of nuclear spillage, natural barriers could act as natural containment barriers via ion-exchange processes and prevent extensive diffusion of harmful elements.

The application of clinoptilolite as a barrier for nuclear waste disposal is supported by its assumed resistance to degradation after γ-radiation. However, data on this topic is rather limited. Fullerton (1961) did not observe changes in the uptake of Na^+, Cs^+, and Ba^+ after γ-radiation of clinoptilolite with a dose of 9.6 Grad, and demonstrated a 42% decrease in the distribution coefficient of clinoptilolite for Ca^{2+} ions after exposure to γ-radiation of 9.6 Grad. Limited information on the stability after irradiation exists also for other zeolites. Pillay and Palau (1982) reported a slight decrease of cation-exchange capacity (CEC) by 3% of a

* E-mail: moraetis@mred.tuc.gr

0003-004X/07/0010–1714$05.00/DOI: 10.2138/am.2007.2545

CHA-type zeolite (chabazite) irradiated with a dose of 5 Grad. In contrast Komarneni et al. (1983) did not observe any decrease of the CEC of CHA-type zeolite after γ-irradiation at a dose of 11 Grad but found an increase of Cs leaching during γ-irradiation while the sample was in contact with water. A decrease in Cs uptake has been reported for zeolite 4A after γ-irradiation with a dose of 0.12 Mrad per hour, associated with a slight decrease in crystallinity and a loss of water content (Daniels and Puri 1986). Obviously, the aforementioned experimental results regarding different rates and doses of radiation are far from being conclusive about the modifications in zeolite structure after irradiation and the subsequent changes in ion-exchange properties.

Notwithstanding the assumed resistance of clinoptilolite and zeolites in general to γ-radiation, detailed studies on the crystal structure of irradiated zeolites are lacking. Moreover, there is lack of published work on the influence of β-radiation on the ion-exchange properties and the structure of zeolites. Important parameters of ion-exchange that may be affected include the equilibrium constant and selectivity for various cations. This lack of information is important because clinoptilolite has been proposed repeatedly in the past for encapsulation of nuclear waste materials, for treatment of liquid nuclear waste, and for remediation of soils contaminated with radionuclides (Smyth 1982; Misaelides et al. 1995a, 1995b; Valcke et al. 1997a, 1997b; Campbell and Davies 1997; Marinin and Brown 2000); however, the long-term stability of clinoptilolite is questionable. The complete understanding of the geochemical behavior upon irradiation is a prerequisite for utilization of zeolites in environmental applications such as nuclear wastewater treatment. Therefore, the aim of the present study was to investigate the effect of irradiation with β- and γ-radiation on the ion-exchange properties of clinoptilolite in systems containing K^+ and Cs^+. Thermodynamic data for ion exchange provide valuable information about ion selectivity after irradiation with β- and γ-radiation. In addition, crystal refinement was attempted to identify crystal changes that may influence ion selectivity.

THEORETICAL CONSIDERATIONS

The exchange reaction between ion $A^{z_A^+}$ (counter-ion) and ion $B^{z_B^+}$ (co-ion) can be written as:

$$z_A B_c^{z_B^+} + z_B A_s^{z_A^+} \Leftrightarrow z_A B_s^{z_B^+} + z_B A_c^{z_A^+} \quad (1)$$

where the subscripts c and s refer to crystal and solution respectively, and z_A, z_B are the valences for the ions A and B, respectively. The equivalent fractions M_A and N_A are defined by

$$M_A = \frac{z_A m_A}{(z_A m_A + z_B m_B)} \quad (2)$$

$$N_A = \frac{z_A n_A}{(z_A n_A + z_B n_B)} \quad (3)$$

where n_A, n_B are the concentration of ions $A^{z_A^+}$, $B^{z_B^+}$ in solution (mol/dm^3), and m_A, m_B are the concentration of the ions in the exchanger (zeolite) (mol/kg) (Dyer et al. 1981).

The rational thermodynamic equilibrium constant is defined by

$$K_\alpha = K_m \Gamma \left(\frac{f_A^{z_B}}{f_B^{z_A}} \right) \quad (4)$$

where K_m is the mass-action quotient of the ion-exchange reaction (Kielland 1935), Γ is the solution phase activity coefficients ratio, ($\gamma_B^{z_A}/\gamma_A^{z_B}$) and f_A, f_B are the activity coefficients of the ions in the zeolite.

The activity coefficient ratio Γ is calculated from the mean activity coefficients of the salts AY and BY

$$\left(\frac{\gamma\pm_{BY_{z_B}}^{z_B^{+1}}}{\gamma\pm_{AY_{z_A}}^{z_A^{+1}}} \right)$$

in mixed electrolyte solution (Robinson and Stokes 1970). The mean activity coefficients γ± are evaluated from the mean molal activity coefficients of each pure salt at the same ionic strength (I) as the mixed electrolyte solution (Glueckauf 1949).

The mass-action quotient is given by

$$K_m = \frac{M_A^{z_B} n_B^{z_A}}{M_B^{z_A} n_A^{z_B}} . \quad (5)$$

The preference of a zeolite for one of the two cations is expressed by the corrected selectivity coefficient K_c (Kielland coefficient) defined by

$$K_c = K_m \times \Gamma. \quad (6)$$

Plots of $\ln K_c$ vs. M_A are used to evaluate the rational thermodynamic constant K_α and the activity coefficients of the ions in the zeolite phase $f_A^{z_B} f_B^{z_A}$ (Gaines and Thomas 1953):

$$\ln K_\alpha = (z_B - z_A) + \int_0^1 \ln K_c \, dM_A \quad (7)$$

$$\ln f_A^{z_B} = (z_B - z_A) M_B + \ln K_c^{(M_A)} + M_A \ln K_c^{(M_A)} + \int_1^{M_A} \ln K_c \, dM_A \quad (8)$$

$$\ln f_B^{z_B} = (z_B - z_A) M_A + M_A \ln K_c^{(M_A)} + \int_0^{M_A} \ln K_c \, dM_A . \quad (9)$$

The standard free energy per equivalent of exchange is given by

$$\Delta G^\circ = \frac{RT}{z_A z_B} \ln K_\alpha \quad (10)$$

where R is the gas constant and T is temperature (K).

The above thermodynamic formulations are valid when salt imbibition is negligible, and water activity makes no contribution in the zeolite. In the present study, the electrolyte concentrations are low (0.025 N) and thus salt imbibition is negligible (Barrer and Walker 1964). The water activity is considered negligible in electrolyte concentrations less than 1 N for both the solution and the exchanger (Barrer and Klinowski 1974). The error introduced by not taking into account the water activity is also negligible (Barrer et al. 1963).

The Kielland coefficient and activity coefficients in zeolite are calculated from normalized values of $M_{Cs,K}$ and $N_{Cs,K}$. Normalization is made by dividing all $M_{Cs,K,Na}$ and $N_{Cs,K,Na}$ values with the maximum value ($M_{Cs,K,Na\ max}$ and $N_{Cs,K,Na\ max}$) calculated by best-fit equation in experimental isotherm points (Loizidou 1982). Superscript N refers to normalized values. Normalization is performed to attain M_A and N_A equal to 1, which are the standard states for both exchanger and solution (Sherry 1966; Dyer

et al. 1981, among many others). In the present study, normalized values were calculated for all data even in cases when M_A equals 1 and N_A does not. Isotherm lines were presented before normalization to facilitate comparison between exchange reactions in different samples.

MATERIALS AND METHODS

Materials characterization and pretreatment

The HEU-type zeolite-rich material was collected from the Republic of Armenia (Nor Kohb deposit in the Noyemberian region). It is a fine-grained, felsic tuff containing 56% HEU-type zeolite, 14% quartz, 7% plagioclase, 7% muscovite, 16% amorphous matter, and traces of smectite (Table 1). Part of the original material (sample N_0) was treated with β- and γ-radiation at the Yerevan Institute of Physics in Armenia and the Institute of Nuclear Chemistry in Italy, respectively. Batches of irradiated material were prepared using three different doses of β-radiation [10^{12} e/cm^2 (sample N_1), 10^{15} e/cm^2 (sample N_2), 3×10^{16} e/cm^2 (sample N_3)] and γ-radiation of 70 Mrad (sample N_4). The quantity of sample N_3 was limited and only few isotherm points were obtained. The materials were dried at 105 °C, ground in a ball mill and subsequently with a pestle and mortar so as to pass through 125 μm sieves, and stored at room temperature in desiccators. Bulk mineralogy of the original and the irradiated zeolitic materials was determined by X-ray diffraction (XRD) using a Siemens D500 XRD operating at 35 kV and 35 mA, with a graphite monochromator, and Cu$K\alpha$ radiation. A 0.02/°2θ scan step and 1 s scan time per step was used at the Technical University of Crete.

HEU-type zeolite chemistry was determined by electron microprobe analysis (EPMA) of carbon-coated polished thin sections, using a JEOL JSM-5600 Scanning Electron Microscope (SEM) equipped with an Oxford Link energy dispersive spectrometer (EDS) at the Institute of Geology and Mineral Exploration of Greece. Analyses were carried out using 90 s livetime, 20 kV acceleration current potential, and 2 nA sample current. In each analysis, the activated area had a diameter of ca. 9 μm. The areas for analysis were selected carefully using back-scattered electron (BSE) images to avoid possible contamination by Ti and Fe oxides and sulfides, and to distinguish coarse-grained minerals (quartz, feldspars) from zeolites. Structural formulae were calculated on the basis of 72 O atoms, making the following assumptions: Si and Al were assigned to tetrahedral sites, and Ca, Mg, Ba, Sr, K, and Na are exchangeable cations. The quality of analyses was evaluated from the charge-balance equation, $E = 100\% \times [Al + Fe - (2Ca + 2Mg + 2Ba + 2Sr + K + Na)]/[2(Ca + Mg + Ba + Sr) + K + Na]$ (Gottardi and Galli 1985; Passaglia and Sheppard 2001). Only those analyses with $E < \pm 10\%$ were considered reliable. The characterization of HEU-type zeolites was based on their Si:Al ratio (Meier and Olson 1992) and on thermal stability tests after successive heating at 550 °C for 16 h (Boles 1972; Alietti 1972).

Bulk chemical analysis of the zeolitic tuff was determined by Energy Dispersive X-ray Fluorescence Sprectroscopy (EDS-XRF), using a Bruker S2 Ranger XRF instrument at the Technical University of Crete. The material was dried at 105 °C, ground in a Tema mill, and passed through a 75 μm sieve. Major elements (Si, Al, Ti, Fe, Mn, Mg, Ca, Na, K, and P) were determined from fused-glass disks. The sample was fused using a mixture of 80% Li-tetraborate and 20% Li-metaborate as flux. The measurements were obtained at 40 kV with an Al filter (500 μm) for the heavier elements (Fe, Mn, Ti, Ca, and K) and at 20 kV for the lighter elements (P, Si, Al, Mg, and Na).

Homoionic Na-HEU-type zeolite was obtained by saturation of the zeolitic material with 1 *M* NaCl solution into polypropylene bottles using a solid mass/solution volume ratio of 1/15 g/mL. The bottles were kept in water bath at 70 °C and the solution was changed daily for eight days (Loizidou 1982). Subsequently the zeolitic material was washed thoroughly until chloride free (electrical conductivity of the supernatant solution was less than 40 μS), dried at 80 °C, and stored in a desiccator. The zeolitic water content was determined for the Na-saturated original zeolite (N_0) and the irradiated samples N_2 and N_4 with thermogravimetric analysis (TGA) in the temperature range 50–400 °C using a heating rate of 10 °/min and an air atmosphere (Perkin Elmer TGA 6).

TABLE 1. Quantitative mineralogical analysis including amorphous determination by Rietveld method (relative standard deviation 5%)

	N_0	N_1	N_2	N_3	N_4
Clinoptilolite	56	55	55	42	56
Quartz	14	13	10	13	10
Albite	7	10	12	8	9
Mica	7	6	8	6	6
Amorphous	16	16	15	31	19

The cation-exchange capacity (CEC) of the non-irradiated HEU-type zeolite (N_0) was determined with three different methods: (1) Saturation with 1 *M* KCl solution, which was changed daily, for eight days at 25 °C, followed by replacement of K^+ with Cs^+ using 1 *M* CsCl (Ming and Dixon 1986; Ming and Boettinger 2001) and measurement of the K^+ index cations. CEC was determined in triplicate (denoted as method I); (2) Saturation with 1 *N* ammonium acetate solution for 10 days at 25 °C followed by distillation in a Kjeldahl microsteam distillation apparatus. During NH_4^+-saturation, the supernatant solution was replaced daily. CEC also was determined in triplicate (denoted as method II); and (3) Microprobe analysis of HEU-type zeolite crystals, which permitted calculation of the structural formulae. CEC was calculated from the CaO, MgO, SrO, BaO, Na_2O, and K_2O concentrations determined by the EPMA analysis (denoted as method III). The CEC obtained with this method will be defined as "apparent CEC" of the HEU-type crystals. The term "theoretical CEC" adopted by Inglezakis (2005) for the CEC determined by EPMA is not considered appropriate, because microanalyses of zeolites are often affected by the presence of other minerals due to analytical constraints, such as the use of a defocused electron beam during analysis and the size of the zeolite crystals, which is often smaller than the excited area. The precision of methods I and II is ±1.2%.

Ion exchange experiments

The ion-exchange experiments were conducted at 25 °C. Initially 1 *N* NaCl, KCl, and CsCl stock solutions were prepared from which batch solutions were produced. Several isotherm points were obtained by equilibrating aqueous binary mixed solutions of different K^+/Na^+ and Cs^+/Na^+ ratios with 0.2 g of Na-homoionic zeolitic material in polyethylene bottles. The normality of all solutions was 0.025 *N*. The suspensions were agitated and left to equilibrate for 8 days under periodic stirring. Kinetic experiments by Pabalan and Bertetti (1994) have shown that ion-exchange equilibrium is approached essentially in 2–3 days. After equilibration, the suspensions were centrifuged and the supernatant solutions were removed to obtain the forward points of the isotherms.

In each isotherm, several reverse points were obtained by replacing 20 cm^3 of the initial suspensions with solutions having a different proportion of the ion in question. The proportions of ions were selected so as to transfer a forward point with low M_A and N_A to a reverse point with high M_A and N_A value and vice versa. This procedure ensured that the isotherm was reversible over the whole range of solution compositions (Loizidou 1982). The suspensions were left 8 days to re-equilibrate, centrifuged, and then the supernatant solutions were analyzed (Fletcher and Townsend 1981).

The exchange level was determined by the difference between the initial and final concentration of the different cations. Determination of Cs^+, K^+, and the index cation (Na^+) was carried out with atomic absorption spectrometry (AAS) using a Perkin-Elmer AAnalyst 100 atomic absorption spectrometer at the Technical University of Crete. The uncertainty in the determination of Cs^+, K^+, and Na^+ was 1, 3, and 1%, respectively, based on the reproducibility of the measurements (3 replicates per measure). All reagents were of analytical grade (Merck).

Crystal-structure refinement

Crystal-structure refinement was applied to all samples (N_0, N_1, N_2, N_3, N_4) exchanged with Cs^+ and in samples (N_0, N_1, N_2, N_4) exchanged with Na^+. Due to an insufficient amount of sample, N_3 was refined only in the Cs-form. The X-ray data were collected in the angular range 5–80 °2θ using a 0.03° step and counting time of 10 s per step using the same diffractometer as for the bulk mineralogical analysis. All samples (N_0, N_1, N_2, N_3, N_4) were previously dried at 105 °C and were refined as polycrystalline materials without using any separation technique. The Rietveld method was applied for refinement of the polycrystalline samples, and four mineral phases (clinoptilolite, quartz, albite, muscovite) were attributed to each sample for the refinement procedure (Finger 1989). Data collection was carried out in a chamber with a controlled relative humidity of 50%. Before crystal-structure refinement, quantitative analysis was applied for the determination of the crystalline phases and the amorphous material present in the samples. Especially for the amorphous determination, a known amount of corundum was added (Hill and Howard 1987; Bish and Howard 1988). The refinement progress was checked by the statistical parameters R_p and R_{pw}.

The HEU-type zeolite was refined in the *C*2/*m* space group. The atomic coordinates were adopted from the structures presented by Petrov et al. (1991,

Inorganic Crystal Structure Database No. 72712) for the Cs^+-exchanged forms and by Cappelletti et al. (1999, Inorganic Crystal Structure Database No. 87846) for the Na^+ exchanged forms. Tetrahedral coordinates were kept constant whereas the scale factor and lattice parameters were refined in each cycle. Cation coordinates and site occupancy for extra framework positions also were refined. The associated crystalline phases were refined using fixed models of albite, quartz and muscovite, whereas cell parameters were refined for each phase. The precision of the quantitative analyses is ±5%.

RESULTS

Material characterization

The average chemical composition (mean of 8 analyses), maximum and minimum values, and standard deviation and structural formulae on the basis of 72 O atoms obtained by EPMA for HEU-type crystals are listed in Table 2. The Si^{4+}/Al^{3+} ratio is greater than 4 (Fig. 1) indicating that that the HEU-type zeolite is clinoptilolite (Coombs et al. 1998). This result is in accordance with the results from heating experiments at 550 °C for 16 h, (data not shown), which yielded a negligible decrease of the (020) diffraction maximum, suggesting that the HEU-type zeolite present is type 3 heulandite, i.e., clinoptilolite (Alietti 1972; Boles 1972). The mean CEC calculated from microanalyses (method III) is 2.29 meq/g, varying between 2.14 and 2.40 meq/g. The main exchangeable cations are Ca and K. β- and γ-irradiation did not affect the XRD pattern of the zeolites, except for sample N_3 as is indicated from the relative abundance of clinoptilolite and amorphous matter (Table 1). In contrast, sample N_3 that was irradiated with the highest β-radiation dose (3×10^{16} e/cm^2), has considerably higher amorphous matter content (31%) and lower clinoptilolite content (42%) than the original tuff. Moreover, it is characterized by a decrease in the intensity of the clinoptilolite diffraction maxima and a hump at 20–30 °2θ, indicative of amorphous material.

The CEC of the original and irradiated HEU-type materials determined by methods I, II, and III is listed in Table 3 in addition to the CEC values normalized to 100% clinoptilolite. The normalized CEC of the original material is 2.43 meq/g, i.e., 6.1% higher than the apparent CEC value obtained from method III. The observed difference is attributed to the limited number of analyses and the errors introduced by such measurements. Relative error for chemical analysis (EDS-SEM) is ±7.67% (mean of 8 analyses), which converts to a CEC standard error of 2.29 ± 0.18 meq/g. The XRD method used for quantitative analyses of the zeolite samples may introduce relative errors of up to ±5%, hence the relative error of method I and II is 1.2%. Overall relative uncertainty for method I and II is 5.14%, which yields standard errors 2.43 ± 0.12 and 2.41 ± 0.12 meq/g (Table 3). The differences in CEC determined by methods I, II, and III can thus be explained by the aforementioned standard errors. For all samples except N_3, irradiation did not affect CEC, since the observed difference (decrease by 1.5%) is similar to the precision of the method (±1.2%). Sample N_3 irradiated with 3×10^{16} e/cm^2 exhibited a remarkable decrease in CEC by 26%. However after normalization of the CEC values to 100% clinoptilolite, of the HEU-type material, an essentially constant CEC for all samples (including sample N_3 is observed) (Table 3).

In sample N_3, the decrease of CEC is associated with a decrease of clinoptilolite content due to amorphization. Hence, the onset of amorphization is between a dose of 10^{15} e/cm^2 (sample N_2) and 3×10^{16} e/cm^2. Wang et al. (2000) detected amorphization in three different zeolites (analcime, natrolite, and zeolite-Y) by applying β-radiation with doses of 7×10^{19}, 1.8×10^{20}, 3.4×10^{20} e/cm^2, respectively. Gu et al. (2000) compared amorphization of zeolite-NaY due to irradiation (using a dose 2.5×10^{21} e/cm^2) with structural collapse due to heating in the same type of zeolite. Note that these doses of β-radiation are considerably higher than those applied in the present work. In a similar study, Nilchi et al. (2003) did not report CEC changes in clinoptilolite treated with γ-radiation at a dose of 20 kGy (=20 Mrad). In the present study, neither amorphization nor a decrease of CEC was observed with γ-irradiation at a dose of 70 Mrad. An important reduction in sorption of Cs followed by increased diffusivity was reported by Daniels and Puri (1986), who irradiated zeolite 4A with a γ-radiation of 100 Mrad.

The chemical composition of the original tuff is (in wt%): SiO_2 65.97, TiO_2 0.29, Al_2O_3 11.44, Fe_2O_3 1.56, CaO 4.19, MgO 0.92, Na_2O 0.62, K_2O 2.11, and LOI 12.53. The chemical

TABLE 2. Average chemical composition and structural formulae of the Armenian clinoptilolite

Oxide% (n = 8)	
SiO_2	63.88
Al_2O_3	12.61
CaO	4.31
MgO	0.59
BaO	–*
SrO	–
Na_2O	1.02
K_2O	0.59
Total	83.00
Structural formulae based on 72 oxygen atoms	
Si	29.32
Al	6.82
Ca	2.12
Mg	0.41
Ba	0.0
Sr	0.0
Na	0.93
K	0.34
E%	7.67
Si^{4+}/Al^{3+}	4.30
CEC meq/g (method III)	2.29

* Not detected.

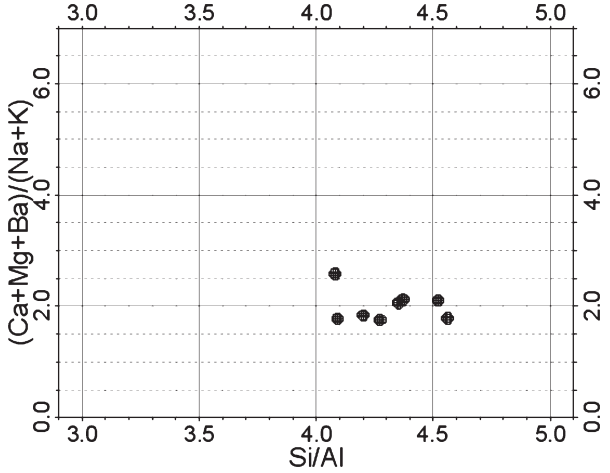

FIGURE 1. Plot of Si^{4+}/Al^{3+} vs. (Ca + Mg + Ba)/(Na + K) showing results for eight (EPMA) analyses of different crystals in the same sample (N_0).

TABLE 3. CEC values obtained, method of determination, clinoptilolite content and normalization of CEC values to clinoptilolite content

Sample	CEC value meq/g (±st. error)	Method	Clinoptilolite content	Normalized values to 100% clinoptilolite
N_0	1.36 (±0.016)	$K^+ \leftrightarrow Cs^+$ (method I)	56% CLN	2.43 (±0.124)
N_0	1.35 (±0.016)	$NH_4^+ \leftrightarrow$ e.c.† (method II)	56% CLN	2.41 (±0.123)
N_0		Chem. anal.‡–EPMA (method III)	100% CLN	2.29 (±0.175)
N_1	1.34 (±0.016)	method I	56% CLN	2.39
N_1	1.34 (±0.016)	method II	56% CLN	*
N_2	1.34 (±0.016)	method I	56% CLN	2.39
N_2	1.27 (±0.016)	method II	56% CLN	*
N_3	1.01 (±0.012)	method I	42% CLN	2.40
N_3	0.98 (±0.011)	method II	42% CLN	*
N_4	1.34 (±0.016)	method I	56% CLN	2.39
N_4	1.27 (±0.016)	method II	56% CLN	*

* No normalization to 100% clinoptilolite since the CEC is the same or lower with this in method I.
† e.c.: exchangeable cations (Na^+, K^+, Mg^{2+}, Ca^{2+}).
‡ Chem. anal.: chemical analysis upon clinoptilolite crystal.

composition is in accordance with the felsic affinities of the tuffs (Petrosov and Sadoyan 1998; Petrosov and Jarbashian 1999). The tuffs are enriched in CaO and K_2O. The large CaO content explains the predominance of Ca as an exchangeable cation in clinoptilolite and the presence of plagioclase, whereas the abundance of K_2O is compatible with the presence of muscovite. The loss of water in the temperature range 50–400 °C for samples N_0, N_2, and N_4 is shown in Figure 2. Samples N_2 and N_0 display identical behavior during heating and lose 8.4 wt% water at 300 °C. Sample N_4 lost 0.45 wt% less water loss than samples N_0 and N_2 at 300 ºC (0.6 wt% at 400 ºC).

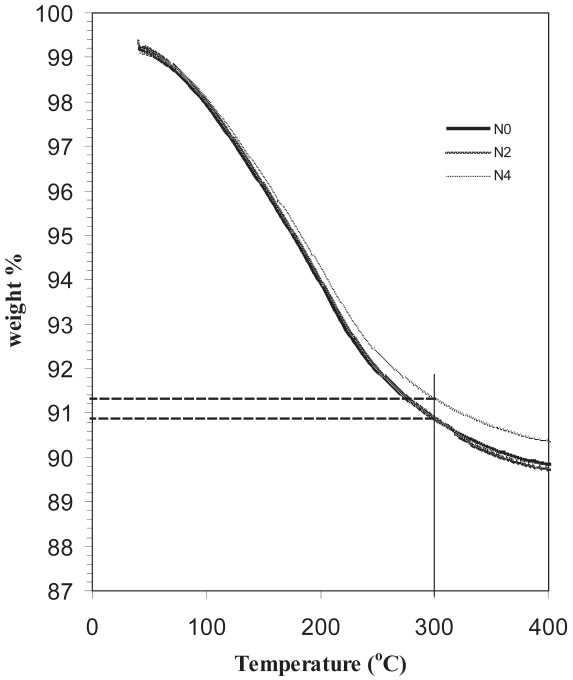

FIGURE 2. Thermal curves of N_0, N_2, N_4 in air heating rate 10 °C/min (TGA).

Ion-exchange isotherms and thermodynamic parameters

The ion-exchange isotherms for the binary systems $K^+ \leftrightarrow Na^+$ and $Cs^+ \leftrightarrow Na^+$ containing forward and reverse points are shown in Figures 3 and 4, respectively. The ion-exchange isotherms are plots of the equilibrium equivalent mole fraction of an exchanging ion in solution vs. the equilibrium equivalent mole fraction of the same ion in clinoptilolite. The best-fit curve was applied to isotherm points by regression analysis. The isotherm curves for both binary systems were fit best by logarithmic equations. The null hypothesis that the fitted line was not randomly selected was examined through ANOVA by F-test (theoretical F/calculated F: 4.3/493 approximately in all cases for significance level 5%). The equilibrium concentrations of each cation in clinoptilolite, X(c), and the solution, X(s), were calculated from the concentrations of both cations involved in each ion-exchange system namely, $K^+ \leftrightarrow Na^+$, and $Cs^+ \leftrightarrow Na^+$. Also, sample weight, solution volume, and CEC were involved in the calculation of cationic mole fractions. The equations used to calculate the cationic mole fraction of an ion in the zeolite and solution are the following:

$$X(\mathrm{c}) = \frac{(X_\mathrm{i} - X_\mathrm{f} \cdot V)}{(X_\mathrm{i} - X_\mathrm{f} \cdot V) + (\mathrm{CEC} \cdot W - Na_\mathrm{f} \cdot V + Na_\mathrm{i})} \quad (11)$$

$$X(\mathrm{s}) = \frac{X_\mathrm{f}}{X_\mathrm{f} + Na_\mathrm{f}} \quad (12)$$

where, X_i, X_f are the initial and final concentration, respectively, of the cation in question in solution (K^+ or Cs^+), and Na_i and Na_f are the initial and final concentrations, respectively, of Na^+ in solution. CEC is the cation-exchange capacity for each sample (cf. Table 3). W and V are the sample weight (g) and the solution volume (mL), respectively.

Equations 11 and 12 are estimated by taking into consideration the concentrations of both the counter-ion and co-ion. Pabalan (1994) mentioned the importance of calculating isotherm points from both the incoming and outgoing concentration because large errors may be introduced especially at the extrema of the isotherm curve. In contrast to the study of Pabalan (1994), in the present case, both concentrations of the counter and co-ion are included in the calculation of one isotherm point (Eqs. 11 and 12).

The observed errors are lower than those estimated by Pabalan (1994). Reversibility is confirmed along the isotherm curves for all the binary systems and all samples. The isotherm lines were well fitted by the logarithmic equation $y = \alpha \ln(x) + \beta$, which was transformed to its linear form $y = a\chi + \beta$. The resultant correlation coefficients, r, range between 0.97 and 0.99, and the coefficients of determination, R, vary between 0.95 and 0.97 for the various samples. This indicates good fitting of the theoretical line calculated by regression analysis. The maximum values for M_K and M_Cs ($M_\mathrm{K}$max and $M_\mathrm{Cs}$max, respectively) were predicted from the best fit line for the thermodynamic calculations and not experimentally, because large errors are involved at the extrema

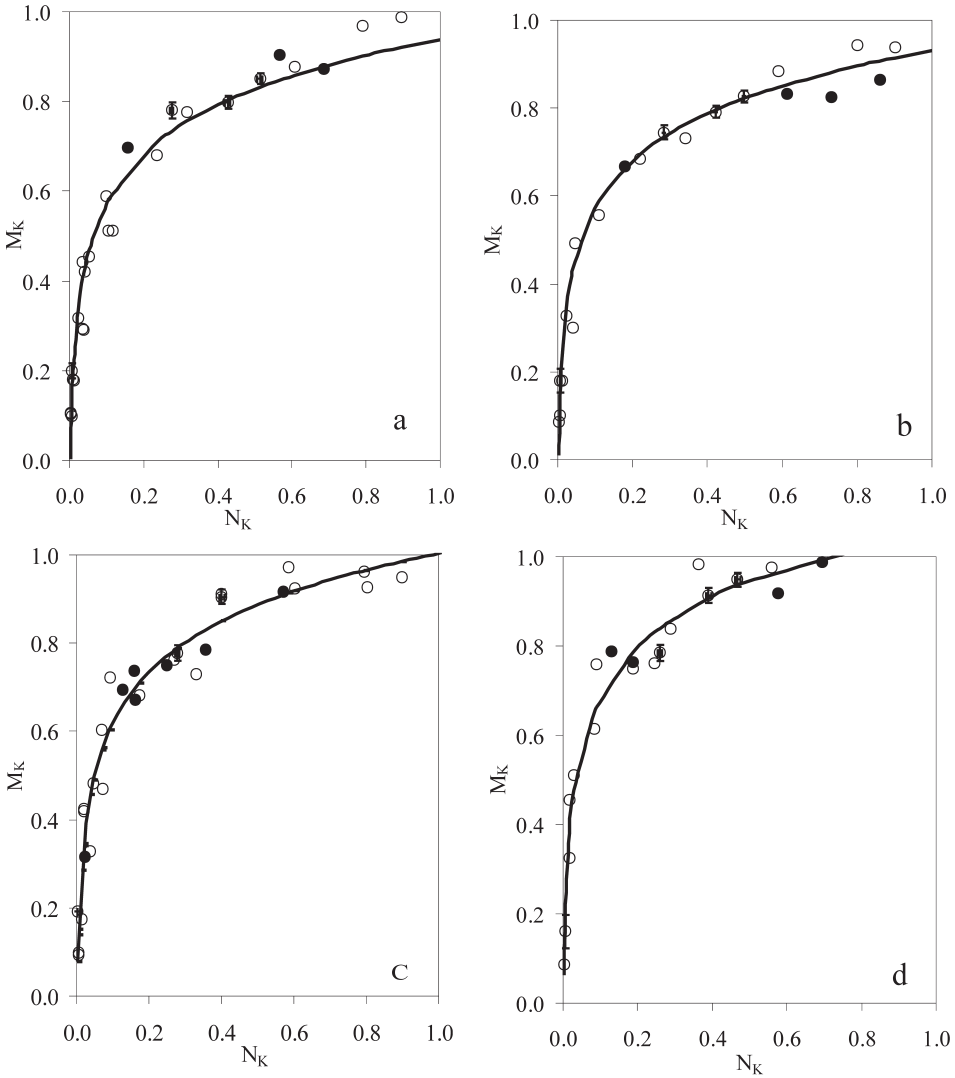

FIGURE 3. Isotherms for $K^+ \leftrightarrow Na^+$ ion exchange at 25 °C with constant normality 0.025 *N*. Open circles correspond to forward points and filled circles to reverse points (**a**) sample N_0, (**b**) sample N_1, (**c**) sample N_2, (**d**) sample N_4. Error bars are presented.

of the isotherms lines (Pabalan 1994).

The isotherm lines for the binary system $K^+ \leftrightarrow Na^+$ and samples N_0, N_1, and N_2 (Figs. 3a, 3b, and 3c), are classified as type 1 according to Colella (1996) or type a according to Breck (1974). All samples exhibit a clear preference for K^+ over Na^+ in accordance with other workers (Ames 1960; Jama and Yücel 1990; Pabalan 1994). The exchange isotherm line for sample N_4 (Fig. 3d) is different from the other samples because it is shifted toward higher M_K as N_K increases. Moreover the maximum load of K^+ was attained much earlier in the isotherm for sample N_4 compared to the other samples. These results suggest a greater preference for K^+ over Na^+ in sample N_4 compared to samples N_0, N_1, and N_2.

The isotherms for the binary systems $Cs^+ \leftrightarrow Na^+$ for samples N_0 and N_1, (Figs. 4a and 4b) are similar to those of the $K^+ \leftrightarrow Na^+$ system for the same samples. In contrast, the isotherms for samples N_2, N_3, and N_4 (Figs. 4c, 4d, and 4e) are similar to sample N_4 for the binary system $K^+ \leftrightarrow Na^+$. Thus, there is a greater preference for Cs^+ in samples N_2, N_3, and N_4 compared to samples N_0, and N_1, and the maximum load of Cs^+ was attained earlier, similar to sample N_4 in the $K^+ \leftrightarrow Na^+$ system.

The activity ratio Γ was calculated for all binary systems, and it was close to unity with no variation with solution composition. This is due to (1) the uni-univalent exchange reaction, and (2) the Extended Debye and Hückel equation (1923) simplified by Güntelberg (1926), which was used for the estimation of the electrolyte mean activity coefficient for each salt in the pure state (Nordstrom and Munoz 1994). The Güntelberg equation (1926)

$$\left(\log \gamma_{\pm AX} = \frac{A \left| z_A z_X \right| \sqrt{I}}{1+\sqrt{I}} \right)$$

is applicable to electrolyte solutions with ionic strengths $I <$ 0.1 at a temperature 25 °C, as is the case in the present study. In the Güntelberg equation, A is a solvent parameter given in

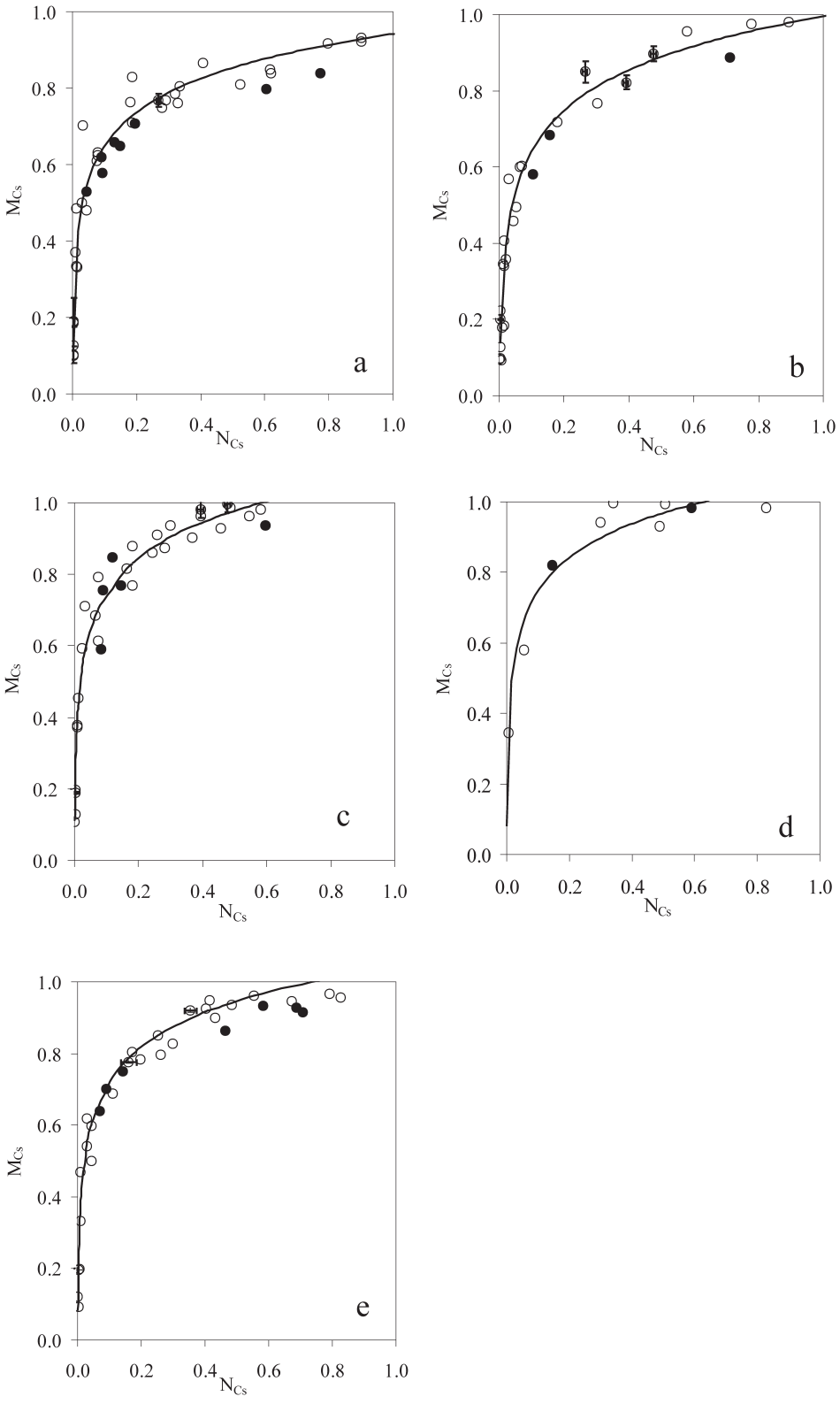

FIGURE 4. Isotherms for $Cs^+ \leftrightarrow Na^+$ ion exchange at 25 °C with constant normality 0.025 *N*. Open circles correspond to forward points and filled circles to reverse points (**a**) sample N_0, (**b**) sample N_1, (**c**) sample N_2, (**d**) sample N_3, (**e**) sample N_4. Error bars are presented.

tables (e.g., Nordstrom and Munoz 1994). The Pitzer model (Pitzer 1991) was not used for simplicity since the Güntelberg modification is well fitted to dilute solutions.

The Kielland plots for all samples in the two binary systems are shown in Figure 5 ($K^+ \leftrightarrow Na^+$) and Figure 6 ($Cs^+ \leftrightarrow Na^+$). With one exception (Fig. 6e), the plots have been modeled by quadratic equations. In the system $Cs^+ \leftrightarrow Na^+$, the Kielland plot of sample N_4 (Fig. 6e) is modeled by a linear equation. Some points do not fit well to the theoretical equations, especially at the extrema of the curves, due to the limited accuracy in determination of K^+, Cs^+, and Na^+ concentration when M_K or M_{Cs} are close to 0 and 1. These observations are in accordance with the results of other workers (Rees 1980; Franklin and Townsend 1985a, 1985b; Jama and Yücel 1990; Pabalan 1994).

In the $K^+ \leftrightarrow Na^+$ exchange, samples N_0, N_1, and N_2 have similar selectivity coefficient plots, which is expected from the similar coefficients of the theoretical quadratic equations (Fig. 5). In contrast, the selectivity coefficient of sample N_4 is clearly different and this is expressed also in the coefficients of the theoretical equation (Fig. 5d). Selectivity for K^+ is greater in sample N_4 compared to the other samples. Hence, in the $K^+ \leftrightarrow Na^+$ system, γ-radiation affected selectivity for K^+, whereas β-radiation did not have a significant influence. In the $Cs^+ \leftrightarrow Na^+$ exchange, irradiation affects selectivity for Cs^+ in all samples as can be observed in the Kielland plots (Fig. 6). Sample N_4 shows a linear Kielland plot. Samples N_2, N_3, and N_4 seem to have a greater selectivity for Cs compared to N_0 and N_1, suggesting that irradiation with β- and γ-radiation had a more profound influence on the $Cs^+ \leftrightarrow Na^+$ system, compared to the $K^+ \leftrightarrow Na^+$ system. For both exchange systems, selectivity for the incoming ion decreases as the equivalent fraction in the crystal is increased, which corresponds to exchange site filling with incoming ions (i.e., Cs^+, K^+).

The rational equilibrium constant (K_α) and the Gibbs free energy of exchange at standard state ($\Delta G°$) for all samples in both systems were calculated by integration of the equations

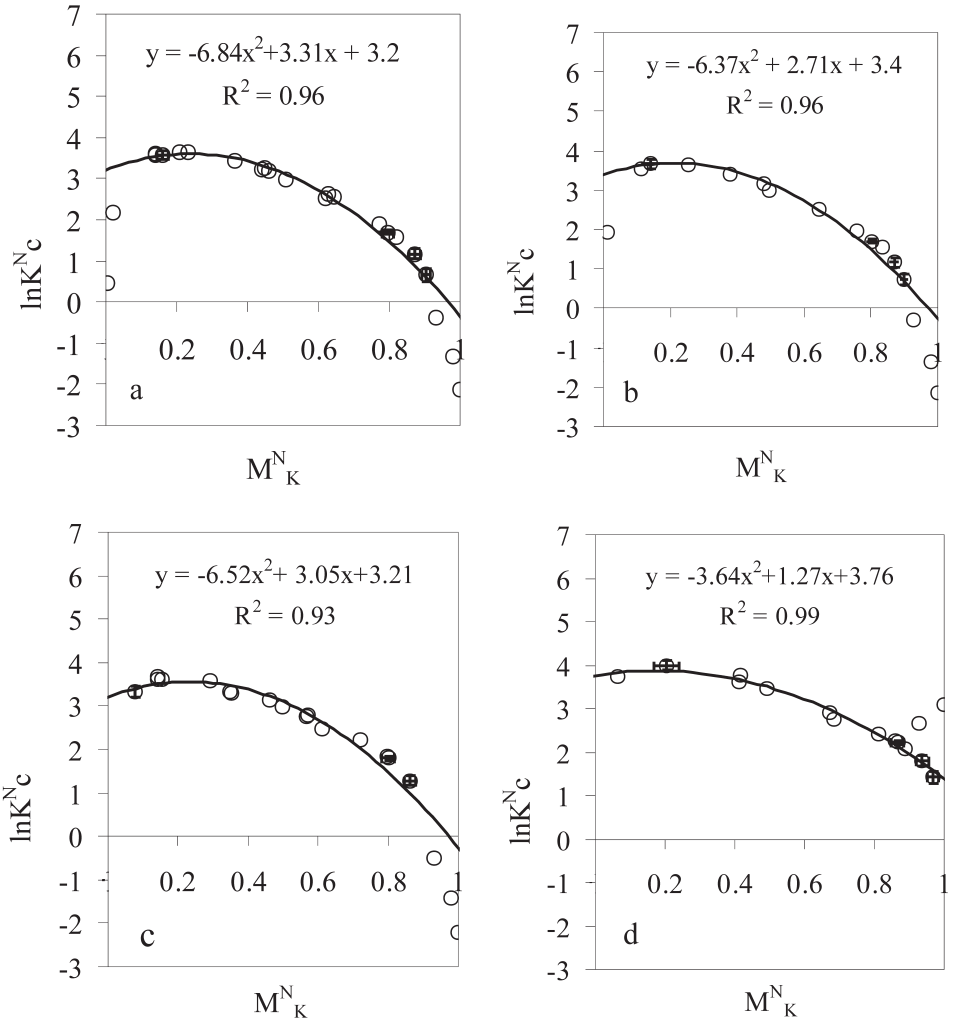

FIGURE 5. Normalized Kielland plots for $K^+ \leftrightarrow Na^+$ exchange against equivalent fraction of K^+ in the original and irradiated clinoptilolite (**a**) N_0, (**b**) N_1, (**c**) N_2, (**d**) N_4. Best-fit curve and curve equation was determined by regression analysis.

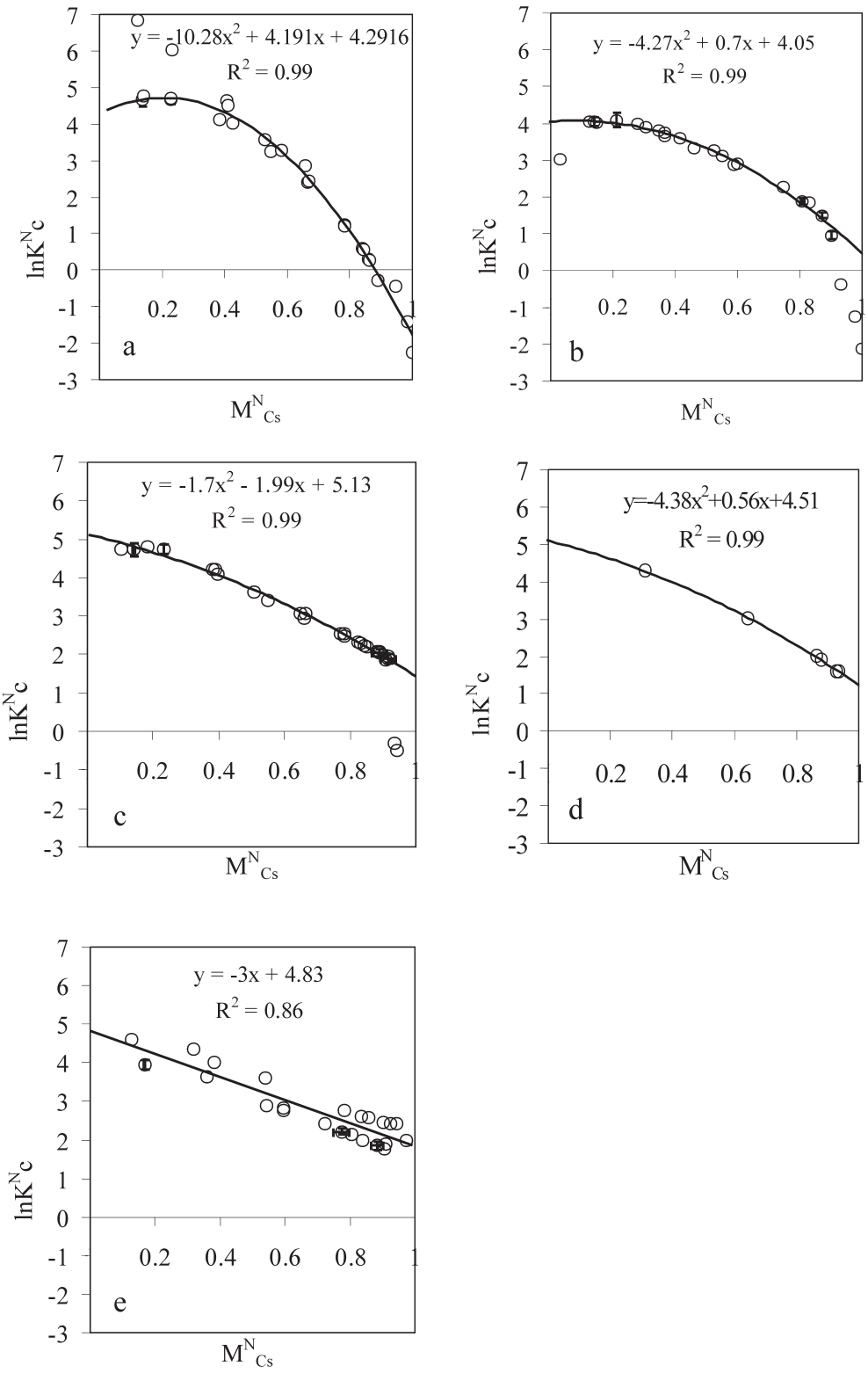

FIGURE 6. Normalized Kielland plot for $Cs^+ \leftrightarrow Na^+$ exchange against the normalized equivalent fraction of Cs^+ in the original and irradiated clinoptilolite (**a**) N_0, (**b**) N_1, (**c**) N_2, (**d**) N_3, (**e**) N_4. Best-fit curve and curve equation was determined by regression analysis.

that model the Kielland plots. The results are listed in Table 4. The results confirm that, in the $K^+ \leftrightarrow Na^+$ system, clinoptilolite irradiated with γ-radiation (sample N_4) exhibits higher selectivity for K^+ compared with the other samples. Moreover, irradiation with β-radiation (samples N_1 and N_2) does not affect selectivity for K^+, because $\Delta G°$ is essentially constant and similar to that of the untreated clinoptilolite (sample N_0). In contrast, selectivity for Cs^+ clearly increases with a gradual increase in the dose of β-radiation compared to the original clinoptilolite (cf. samples N_1, N_2 compared to sample N_0). A further increase of irradiation dose (sample N_3) is not followed by an increase in the selectivity for Cs^+. The thermodynamic parameters obtained for the $K^+ \leftrightarrow Na^+$ exchange in the untreated clinoptilolite (sample N_0) are similar to those reported by Ames (1964) ($\ln K\alpha = 2.54$, $\Delta G° = -6.29$ kJ/mol). The apparent difference with the results of Pabalan (1994) is explained by the different activity coefficient model used in that study. In the system $Cs^+ \leftrightarrow Na^+$, the thermodynamic parameters for original clinoptilolite N_0 are different from those reported by Ames (1964). Since Ames (1964) used the same material for both exchange reactions, and his results are similar to our results only for the $K^+ \leftrightarrow Na^+$ system, it is suggested that the normalization procedure probably affected the thermodynamic results for the $Cs^+ \leftrightarrow Na^+$ exchange (Dyer et al. 1981; Franklin and Townsend 1985a, 1985b). Despite the observed difference with the results of Ames (1964), the well-known selectivity order of Cs > K > Na is obvious for the untreated clinoptilolite (Ames 1960; Chelishchev et al. 1973).

The activity coefficients for K and Cs for the $K^+ \leftrightarrow Na^+$ and $Cs^+ \leftrightarrow Na^+$ exchange are presented in Figures 7 and 8, respectively. $K^+ \leftrightarrow Na^+$ exchange is characterized by similar activity coefficient plots in all samples. The activity coefficient plots for $Cs^+ \leftrightarrow Na^+$ exchange are more sigmoidal compared to the $K^+ \leftrightarrow Na^+$ plots. As expected, when the activity coefficients of K^+ or Cs^+ are maximized, the Na^+ ion activity coefficients are minimized.

Structure refinement of the Na- and Cs-exchanged samples

The lattice parameters of the refined samples are listed in Table 5 and results from extraframework cation position and occupancy refinement are shown in Table 6. The Cs^+-exchanged original clinoptilolite (N_0) has a larger b_o lattice parameter (average increase 0.110 Å) compared to its Na^+-exchanged counterpart. Yang and Armbruster (1996) observed an increase in lattice parameters of 0.164 Å for the Cs^+-exchanged clinoptilolite, and similar observations were made by Petrov et al. (1991). A volume increase is related to cation radii. In contrast, the crystallographic parameters of Na^+-exchanged sample N_0 are essentially the same as those of the initial structural model (87864). The Na-saturated irradiated samples (N_1, N_2, and N_4) display a slight increase in volume compared to the original sample N_0. In contrast, changes in extraframework positions for the irradiated samples N_1, N_2, N_4, and occupancy were not observed. The statistical values R_p and R_{wp} in Rietveld refinement indicate a good agreement between the theoretical and calculated intensity values. Observed differences for R_p and R_{wp} between the theoretical models (87864, 72712) and present refinement results are mainly due to lower accuracy observed in polycrystalline crystal refinements. The extraframework sites Na1, Na2, Na3, and Na4, are correlated with sites M1, M2, M3, and M4 of Koyama and Takeuchi (1977). Position Na4 is not occupied in the present study and this was also observed by Smyth et al. (1990) and Cappelletti et al. (1999). The Na4 (M4) position can be occupied by Mg^{2+}, which can be distributed over other extraframework positions (Cappelletti et al. 1999).

The lattice parameters were not affected for N_0, N_2, N_3, and N_4 Cs-saturated clinoptilolite. The statistical values R_p and R_{wp} are similar to those obtained for refinement of Na-exchanged clinoptilolite. The exchangeable sites occupied by Cs^+ determined in the present study (Cs1, -Cs2, -Cs3, and -Cs4) coincide with those determined by Smyth et al. (1990) (M3, M4, M1, M2, respectively), and by Yang and Armbruster (1996) (*C*3, *A*2, *A*'2, *B*4, respectively). The fifth Cs^+ position (M5) observed by Smyth et al. (1990) was not refined in this study following the crystal structure model of Petrov et al. (1991). Refinement of Cs positions for samples N_2, N_3, and N_4 showed shifts in x and z coordinates for the cation site Cs2 and a concomitant decrease of occupancy. In particular, sample N_3 displays a maximum decrease in occupancy of cation site Cs2 (20%), which is not in accordance with the CEC measurements for the pure clinoptilolite in the same sample. Normalized CEC determined by method I for sample N_3 (Table 3) is essentially identical to the original sample (N_0). The fact that the decrease in occupancy of a cation site in sample N_3 was not accompanied by a CEC decrease is attributed either to cation sites, that were not determined, like M5 (Smyth et al. 1990), or to additional exchange sites formed during irradiation. Cappelletti et al. (1999) observed discrepancies between the CEC determined experimentally and that determined by crystal structure refinement. Cation site Cs3 exhibited changes in x and z coordinates for the irradiated samples N_2 and N_3 but not for sample N_4. In a similar study, Daniels and Puri (1986) related the decrease of Cs^+ sorption by irradiated zeolite 4A (dose 120 Mrad) to the collapse of cation exchange sites due to amorphization. Although we did not trace significant modifications in Cs^+-exchange sites after γ-irradiation with 70 Mrad, a higher dose of γ-radiation (e.g., 120 Mrad) may affect the exchange sites of clinoptilolite.

TABLE 4. Thermodynamic results for exchange $K^+ \leftrightarrow Na^+$, $Cs^+ \leftrightarrow Na^+$ for the samples N_0, N_1, N_2, N_3, N_4

Samples	ln*Kα* at 298 K	Δ*G*° (kJ/equiv)
	$K^+ \leftrightarrow Na^+$	
N_0	2.58	–6.37
N_1	2.61	–6.47
N_2	2.56	–6.34
N_4	3.18	–7.88
	$Cs^+ \leftrightarrow Na^+$	
N_0	2.96	–7.33
N_1	2.99	–7.41
N_2	3.57	–8.83
N_3	3.47	–8.60
N_4	3.33	–8.25

DISCUSSION

Cation exchange capacity of clinoptilolite

Determination of CEC is of major importance for thermodynamic calculations because it corresponds to the maximum exchange that can be attained by the zeolite, and it is used for

TABLE 5. Lattice refinement parameters for Na^+, Cs^+-loaded samples

Samples	a_o (Å)	b_o (Å)	c_o (Å)	β (°)	V (Å^3)	R_{wp}*	R_p†
Na^+-exchanged samples							
Th. model (87864)	17.674(3)	17.957(3)	7.409(1)	116.30(4)	2108.11(6)	7.1	5.6
N_0	17.654(4)	17.965(4)	7.409(1)	116.29(1)	2107.03(77)	17.47	13.60
N_1	17.667(4)	17.976(4)	7.412(1)	116.33(2)	2110.06(81)	17.43	13.84
N_2	17.668(4)	17.977(4)	7.412(1)	116.31(2)	2110.49(80)	17.17	13.74
N_4	17.670(4)	17.976(4)	7.413(2)	116.30(2)	2110.79(84)	16.40	12.87
Cs^+-exchanged samples							
Th. model (72712)	17.744(6)	17.987(5)	7.426(2)	116.01(2)	2130(1)	0.052	0.031
N_0	17.761(7)	18.073(8)	7.430(3)	115.740(1)	2152.5(17)	16.59	13.36
N_2	17.751(78)	18.074(7)	7.439(1)	116.65(16)	2151.4 (18)	16.53	13.23
N_3	17.781(3)	18.090(4)	7.466(1)	116.15(2)	2156.49(80)	13.3	10.35
N_4	17.756(7)	18.072(4)	7.436(2)	115.94(2)	2145.7(16)	16.08	12.84

Notes: Y_{io} and Y_{ic} are the experimental and the calculated intensity for each diffraction peak. w_i is the relative standard deviation for each refined peak.

* $R_{wp} = \left[\Sigma w_i \left(Y_{io} - Y_{ic}\right)^2 / \Sigma w_i Y_{io}^2\right]^{1/2}$.

† $R_P = \Sigma\left|Y_{io} - Y_{ic}\right| / \Sigma Y_{io}$.

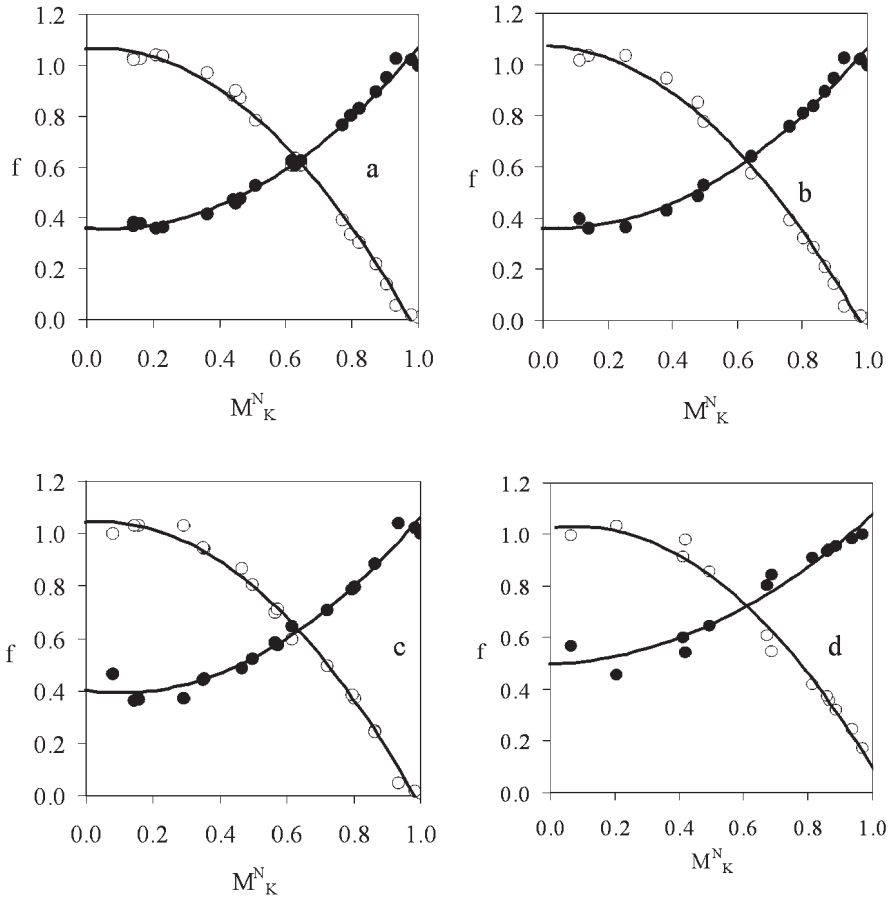

FIGURE 7. Activity coefficients of K^+ (closed circles) and Na^+ (open circles) in the zeolite phase vs. equivalent fraction (normalized) of K^+ in the original and irradiated clinoptilolite (**a**) N_0, (**b**) N_1, (**c**) N_2, (**d**) N_4. Gaines and Thomas (1953) equations applied.

normalization of isotherm data. Therefore, reliability of CEC results is important for the credibility of the thermodynamic study of ion exchange. Several workers (Lehto et al. 1995; Inglezakis 2005, among others) have discussed the different types of capacity used in the literature and different methods of CEC determination. Two points must be clearly stated during CEC determination. First, the percentage and type of impurities present in the sample, if any, and second, the method of CEC determination. When comparing CEC values, it is useful to compare clinoptilolite content and the method of determination, and then the Si^{4+}/Al^{3+} ratio (Gottardi and Galli 1985) and the physical state of zeolitic material (Jastrezbski 1987; Inglezakis et al. 1999). Faghihian et al. (1999) obtained CEC values of 1.42, 1.24, and 1.44 meq/g for three zeolitic tuffs with a clinoptilolite content of 90–95% using NH_4^+ as the index cation. However, the CEC calculated from the sum of the exchangeable cations (chemical analyses, method not mentioned) was 2.335, 2.096, and 2.357 meq/g, respectively, for the same clinoptilolites. It

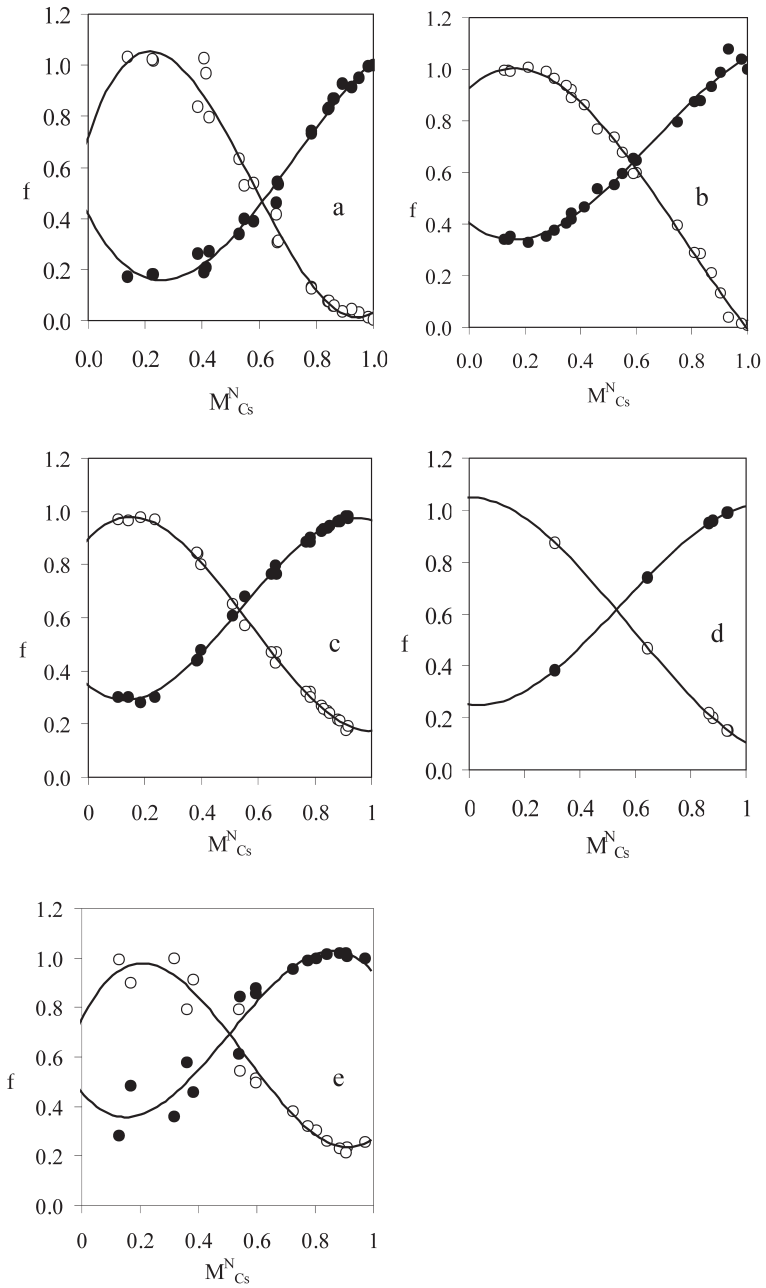

FIGURE 8. Activity coefficients of Cs^+ (closed circles) and Na^+ (open circles) in the zeolite phase vs. equivalent fraction (normalized) of K^+ in the original and irradiated clinoptilolite (**a**) N_0, (**b**) N_1, (**c**) N_2, (**d**) N_3, (**e**) N_4. Gaines and Thomas (1953) equations applied.

is obvious that even after normalization to 100% clinoptilolite content, the calculated CEC (~1.4–1.6 meq/g) is substantially lower than the CEC determined by chemical analysis. This is a typical example in which the CEC obtained by chemical analysis (apparent exchange capacity as explained previously) does not coincide with the CEC obtained using index cations. In other reports, the discrepancy between apparent CEC and the CEC determined by the use of index cations is smaller but still exists (Cerri et al. 2002; Inglezakis et al. 2003). The differences observed in the aforementioned studies between apparent CEC and CEC determined by index cations has been attributed to incomplete exchange of Na with cations (K^+ Ca^{2+}, Mg^{2+}) occupying sites such as M2 or M3 (after Koyama and Takeuchi 1977) (e.g., Inglezakis et al. 2003).

In the present study, the apparent CEC determined by method III is slightly lower than the real CEC determined by method I and/or method II after normalization to 100% clinoptilolite content (Table 3). As noted above, this difference is attributed to the small number of microanalyses and the small size of clinoptilolite crystals (in fact often smaller than the electron

TABLE 6. Refinement results for the cation exchange positions and occupancy (standard deviations in parentheses)

Cation position	x	y	z	occ
		N_0, N_1, N_2, N_4		
Na1	0.1380	0.0000	0.6920	0.34
Na2	0.0470	0.5000	0.1960	0.48
Na3	0.2420	0.5000	0.0410	0.48
Na4	0.0000	0.0000	0.5000	0.00
		N_0		
Cs1	0.2252(13)	0.5000	–0.005(29)	0.600(19)
Cs2	0.0625(19)	0.0000	0.7684(49)	0.400(18)
Cs3	0.0494(15)	0.0000	0.1798(43)	0.400(20)
Cs4	0.0000	0.5000	0.5000	0.600(26)
		N_2		
Cs1	0.2238(13)	0.5000	0.9944(35)	0.600(16)
Cs2	0.0233(19)	0.0000	0.7888(48)	0.373(19)
Cs3	0.0673(21)	0.0000	0.1944(52)	0.400(18)
Cs4	0.0000	0.5000	0.5000	0.600(23)
		N_3		
Cs1	0.2264(14)	0.5000	0.9971(34)	0.599(20)
Cs2	0.0444(26)	0.0000	0.8116(62)	0.323(19)
Cs3	0.0673(21)	0.0000	0.1859(50)	0.400(18)
Cs4	0.0000	0.5000	0.5000	0.600(23)
		N_4		
Cs1	0.2232(12)	0.5000	1.0000(27)	0.599(20)
Cs2	0.0513(25)	0.0000	0.8264(62)	0.282(16)
Cs3	0.0412(16)	0.0000	0.1805(41)	0.400(17)
Cs4	0.0000	0.5000	0.5000	0.600(24)

beam), because of the scarcity of pure clinoptilolite crystals of suitable size. Note that the use of index cations with lower selectivity than Cs^+ or K^+, such as Na^+, often yields lower CEC than the apparent CEC (Langela et al. 2000). In fact, the use of Cs^+ as an index cation after saturation with K^+ (Ming and Dixon 1986) overcomes possible selectivity drawbacks (Ames 1960; Chelishchev et al. 1973). Since the CEC determined by index cations for which clinoptilolite shows high selectivity (Cs^+, NH_4^+) is similar to the apparent CEC, it is likely that the CEC values obtained for pure Armenian clinoptilolite is the real CEC of the mineral. Therefore, the thermodynamic calculations, which were based on a certain maximum cation occupancy calculated from the CEC are sound.

Methods I and II yielded identical CEC values for sample N_0, suggesting that both methods are sufficient for CEC determination of clinoptilolite (Table 3). Similar results were obtained also for sample N_1. The lower CEC obtained with NH_4^+-exchange in samples N_2, N_3, and N_4 reflects probable changes in NH_4^+ selectivity after irradiation, which either hindered NH_4^+ accessing exchangeable sites, thus causing slower kinetics or rendered certain sites inaccessible for NH_4^+ but not for K^+. Such changes are discussed below. In sample N_3 the lower CEC is due to amorphization of clinoptilolite as noted above.

Correlation of crystallographic and thermodynamic results

The observed changes in thermodynamic parameters of ion exchange in the irradiated samples are related to modifications in the clinoptilolite structure. The additional mineralogical phases present in minor or trace amounts (quartz, muscovite, plagioclase) do not affect ion exchange. The main modifications in crystal structure observed during Rietveld refinement of the Cs-saturated samples include decrease of the occupancy of the Cs2 site and shift of the extraframework Cs2 and Cs3 sites toward channel walls as indicated by their coordinates. Another modification observed at more intense irradiation conditions is partial amorphization of clinoptilolite observed in sample N_3.

The cation sites Cs2 and Cs3 are identical to sites *A*2, *A*'2 of Yang and Armbruster (1996) and both sites are coordinated by four O atoms of the framework. Also, according to the aforementioned authors, Cs1 resembles cation site *C*3 in the C-ring and it is coordinated by six framework O atoms. Consequently, site Cs1 is more preferable compared to site Cs2, and it is ideal to compensate the negative charge on the ring walls since it is situated near the framework tetrahedral T2 site, which exhibits greater possibility of Al^{3+} for Si^{4+} substitution (Fig. 9a). The observed population decrease in site Cs2 suggests that the fraction of the more preferable sites (like Cs1) to the total available sites may have increased, because CEC does not decrease significantly so as to explain the observed decrease in occupancy of site Cs2, and so may have the selectivity for Cs^+. The occupancy of Cs1 did not change, indicating either that new sites may have formed or that Cs resides in site M5 (Smyth et al. 1990). However, we were not able to refine such sites with the Rietveld method.

An alternative explanation for the increase of Cs^+ selectivity is that cation sites Cs2 and Cs3 shift toward the channel walls, as indicated by changes in site coordinates after irradiation (Table 6, Fig. 9b). Such changes are expected to cause stronger interaction between the tetrahedral O atoms in the channel walls and extraframework cations, and/or structure bends and deformities near Cs2 and Cs3 and thus increase selectivity for Cs. Previous studies on the effects of irradiation on the structure of different zeolites and clays have considered the role of products of radiolysis of water in the crystal structure of these minerals or the role of Compton scattering, mainly in structural oxygen (Liu and Thomas 1995; Zhang et al. 1998). Irradiation products due to water radiolysis include H_2O^+, H_3O^+, H_2O_2, electrons, hydroxyl, and hydrogen radicals that readily offer electrons due to their excited state from irradiation (Spinks and Woods 1990).

Published data on electrons nesting inside the zeolite structure (Liu et al. 1995) show that long-lived electrons may be trapped into extraframework cation clusters or into water molecules (Liu and Thomas 1995; Zhang et al. 1998). The trapped electrons counterbalance part of the positive charge in exchangeable cations with concomitant decrease of interaction between cations and structure. Had it been the case in our samples, they would have been replaced during Na-saturation because the incoming Na is expected to replace cations with trapped electrons. Gournis et al. (2001) suggested the possibility for the existence of positive charge holes created in framework O atoms in smectite clays due to Compton scattering. Such positive charge holes could have been formed within clinoptilolite, but then the total structural charge would have been lower. This, in turn, would have yielded a lower CEC and weaker attractive forces and hence a lower cation selectivity. However, the CEC of the irradiated samples is essentially the same as that of N_0. Also, the selectivity for Cs^+ is higher for the irradiated clinoptilolite crystals (samples N_2, N_3, N_4) compared to the untreated clinoptilolite (N_0). Thus, change of structural charge is not considered to be a main effect of irradiation that would influence Cs^+-selectivity.

Daniels and Puri (1986) suggested that free radicals (like OH^-, O_2^-) cause displacement of Na^+ and a partial breakup of several structure bonds in synthetic zeolite-4A, thereby increasing specific surface area and causing structure deformities. Moreover, redistribution of hydroxyl radicals with concomitant formation

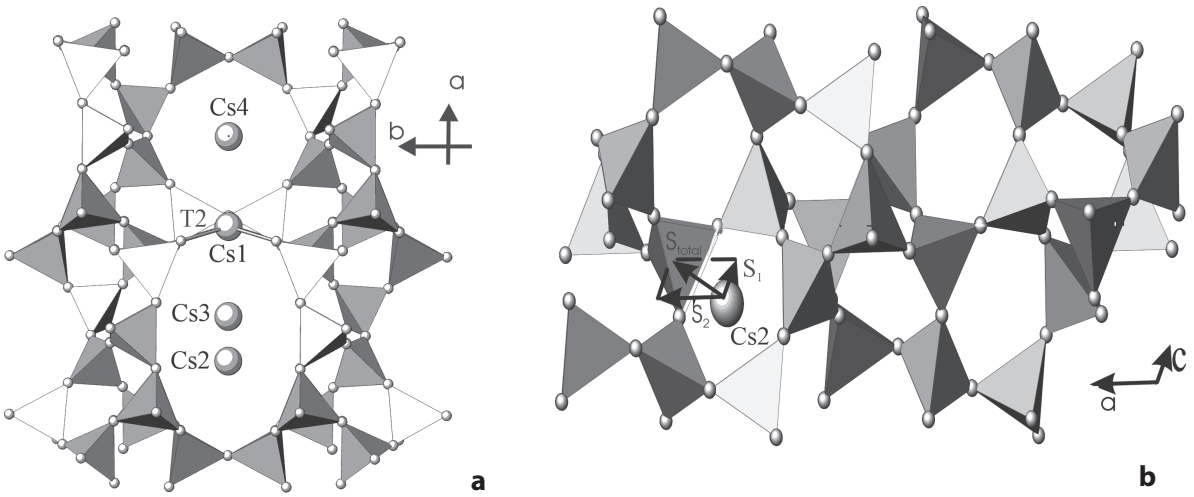

FIGURE 9. (**a**) Schematic representation of the clinoptilolite channels with the location of the various exchange sites and the T2 site. Projection along (001), (**b**) schematic representation of the shift of Cs2 site toward the channel walls of clinoptilolite after irradiation with β- and γ-radiation. S1 and S2 represent shift along *c* and *a* axes respectively. Projection along (010).

of water and hydrogen during irradiation could influence Al coordination and structural deformities may appear (Ermatov et al. 1980; Zhang et al. 1998). Irradiation with γ-radiation has been found to increase the intensity of the vibrations of the outer Al-O and Si-O bonds in infrared spectra of zeolite-NaA, suggesting a greater bond distance, and hence a more loose structure (Ermatov et al. 1980). Such effects probably favor the shift of Cs2 and Cs3 sites toward channel walls and the observed increase of Cs^+-selectivity, and/or also could cause structure deformations, which bend channel walls toward Cs2 and Cs3.

It has already been mentioned that amorphization is commonly observed during irradiation of zeolites. Acosta et al. (1993) detected lower CEC in zeolite CaA after irradiation with β-radiation, which was attributed to the collapse of the channel opening due to amorphization and "locked-in" exchangeable cations. This is not considered probable in the present study since the blocked channel entrances would have impaired Cs^+ exchange and CEC would have been lower for the irradiated samples, which was not the case. A more plausible mechanism for amorphization is the production of hydrogen ions and highly energetic radicals, such as OH^- (Wang et al. 2000), during radiolysis of water. This may facilitate zeolite dissolution through attack on Al-O-Si bonds with possible removal of exchangeable cations (Fig. 10). Such a mechanism can be considered as the next step in the formation of longer Si-O and Al-O bonds mentioned before, and is similar to the role of H ions in acid solutions, which also cause amorphization (Casey et al. 1988; Ragnarsdóttir et al. 1993; Yamamoto et al. 1996). Extraframework cation mobility due to free radicals resembles heat-collapsed structures studied by Alberti and Vezzalini (1983). The Cs2 and Cs3 sites involve weaker attraction forces between exchangeable cations and structure walls and probably the cations hosted there are more prone to mobility due to shift of free radicals. A similar behavior has been observed by several researchers during dehydration of clinoptilolite, in which the cations situated in sites like Na1 and Ca2 slowly shifted as dehydration proceeded, whereas K3 remained intact to preserve the channels (Koyama and Takeuchi 1977; Armbruster and Gunter 1991).

An alternative possibility for the observed differences in the thermodynamic parameters of clinoptilolite during ion exchange may be related to variations in the water content of the various types of clinoptilolite studied. Sample N_4 has slightly lower zeolitic water content than samples N_0 and N_2 (Fig. 2). A lower water content in the zeolite channels would increase free space, hence facilitating diffusion of incoming cations in the exchangeable sites, and thus might explain the observed decrease of $\Delta G°$ of ion exchange in the irradiated samples. However, the lower zeolitic water content of sample N_4 (by 0.45 wt%, corresponding to 5% relative decrease compared to the original sample) is not enough to account for the observed decrease in $\Delta G°$ (24% compared to the original sample). Most important is the fact that in the $Cs^+ \leftrightarrow Na^+$ exchange, sample N_2 displays a maximum decrease in $\Delta G°$ although it has a water loss identical to that of the original clinoptilolite. The small differences in water content between N_0 and N_4 can be attributed to inhomogeneity in the zeolitic tuff. This suggests that the differences in zeolitic water content are not decisive for the observed differences in $\Delta G°$ and ion selectivity. Refinement of water positions could yield interesting results in the role of water in such systems but this was not possible in the present study, given sample purity and other physical characteristics.

We cannot discuss possible structural changes in K-exchanged samples after irradiation with β- and γ-radiation since there are no Rietveld refinement results for the irradiated samples. An increase in K^+ selectivity was observed after irradiation with γ-radiation similar to Cs^+. The changes in ion exchange induced by β-radiation are probably related also to the cation involved in the reaction, since β-irradiation affected only the $Cs^+ \leftrightarrow Na^+$ reaction and not $K^+ \leftrightarrow Na^+$. Probably the cation sites that preferably host K have not been seriously affected by β-radiation. According to our results, the Cs2 site seems to bear the most extensive changes after irradiation of clinoptilolite. The same

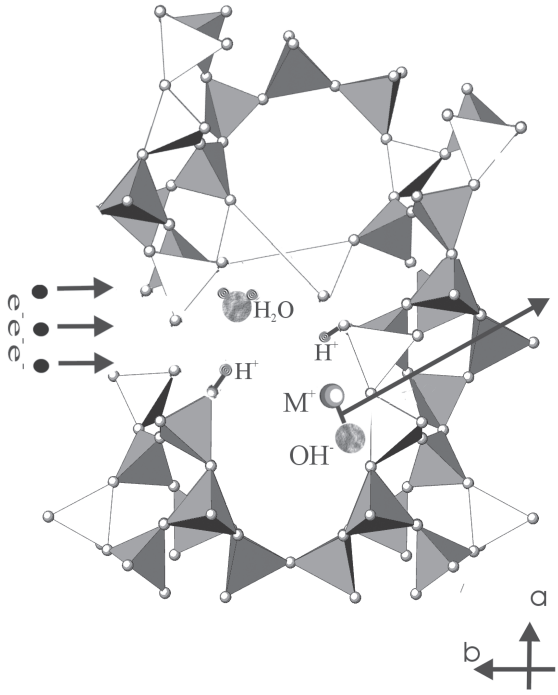

FIGURE 10. Schematic diagram for the disruption of clinoptilolite framework after irradiation. Modified after Wang et al. (2000).

site resembles *A2,* which is not preferred by K^+ (Yang and Armbruster 1996). In contrast, irradiation with γ-radiation seems to introduce changes for both ion-exchange reactions, suggesting that the changes imposed are not sensitive to the type of cation involved in the reaction.

Cation-exchange capacity is not the only parameter to be considered when assessing the influence of irradiation on the clinoptilolite structure. An increase of selectivity for Cs^+ and K^+ after irradiation with γ-radiation and/or β-radiation without remarkable changes in CEC capacity was observed. Although clinoptilolite is considered, in general, a resistant material during irradiation, this does not seem to be the case when investigating the thermodynamics of ion-exchange reactions. Structure deformation and finally collapse with increasing intensity of β-radiation occurs with concomitant increase of the amount of amorphous material. Clinoptilolite structure modifications are centered in the vicinity of Cs2 and Cs3 sites, which hold exchangeable cations with weaker forces. The mobility of the weakly held cations increased due to water radiolysis and induced structural changes, which increased selectivity for cations like Cs^+.

A combination of Rietveld refinement results and thermodynamic calculations may assist in understanding the influence of irradiation on solids. The results of the present study are important for projects on nuclear waste treatment because they can allow an assessment of environmental risk for long- and intermediate-lived radionuclides storage. For instance, the influence of the decay products of radionuclides adsorbed by the zeolites in radioactive waste-water treatment (these involve β- and γ-radiation) can be assessed, especially when considering that this influence is additive. By taking into account storage time spans of zeolites loaded with radionuclides, an assessment of irradiation dose would predict possible changes in the clinoptilolite structure and the ion-exchange properties. An interesting aspect would be the investigation of the state of adsorbed radionuclides after amorphization of clinoptilolite. Sorption behavior and diffusion of radionuclides through irradiated clinoptilolites needs further consideration in view of the present results.

ACKNOWLEDGMENTS

This work was funded by the Greek Scholarship Foundation (SSF) (contract no. 34/2000-01) and by EU (INCO-Copernicus Project, contract no. ICA-CT-2000-10019). The constructive comments of R.T. Pabalan and P.S. Neuhoff improved the text.

REFERENCES CITED

Abusafa, A. and Yücel, H. (2002) Removal of ^{137}Cs from aqueous solutions using different cationic forms of a natural zeolite: clinoptilolite. Separation and Purification Technology, 28, 103–116.

Acosta, D.R., Vazquez-Polo, G., Garcia, R., and Castano, V.M. (1993) Electron beam degradation of Ca-A zeolite. Radiation effects and defects in solids, 127, 37–43.

Alberti, A. and Vezzalini, G. (1983) The thermal behaviour of Heulandites: A structural study of dehydration of Nadap Heulandite. Tschermaks Mineralogische and Petrographische Mitteilungen, 31, 259–270.

Alietti, A. (1972) Polymorphism and crystal-chemistry of heulandites and clinoptilolites. American Mineralogist, 57, 1448–1462.

Ames, L.L. (1960) The cation sieve properties of clinoptilolite. American Mineralogist, 45, 689–700.

——— (1964) Some zeolite equilibria with alkali metal cations. American Mineralogist, 49, 127–145.

Armbruster, T. and Gunter, M. (1991) Stepwise dehydration of heulandite-clinoptilolite from Succor Creek, Oregon, U.S.A. A single-crystal X-ray study at 100 K. American Mineralogist, 76, 1872–1883.

Barrer R.M. and Klinowski, J. (1974) Ion-exchange selectivity and electrolyte concentration. Journal of the Chemical Society Faraday Transactions 1, 70, 2080–2091.

Barrer, R.M. and Walker, A.J. (1964) Imbibition of electrolytes by porous crystals. Transactions of the Faraday Society, 60, 171–184.

Barrer, R.M., Rees, L.V.C., and Ward, D.J. (1963) Thermochemistry and thermodynamics of ion exchange in a crystalline exchange media. Proceedings of the Royal Society of London Series A, 273, 180–197.

Bish, D.L. and Howard, S.A. (1988) Quantitative phase analysis using the Rietveld method. Journal of Applied Crystallography, 21, 86–91.

Bodvarsson, G.S., Boyle, W., Patterson, R., and Williams, D. (1999) Overview of scientific investigations at Yucca Mountain—the potential repository for high-level nuclear waste. Journal of Contaminant Hydrology, 38, 3–24.

Boles, J.R. (1972) Composition, optical properties, cell dimensions and thermal stability of some heulandite group zeolites. American Mineralogist, 57, 1463–1493.

Breck, J.R. (1974) Zeolite Molecular Sieves: Structure, Chemistry, and Use. Wiley, New York.

Campbell, L.S. and Davies, B.E. (1997) Experimental investigation of plant uptake of cesium from soils amended with clinoptilolite and calcium carbonate. Plant and Soil, 189, 65–74.

Cappelletti, P., Langella, A., and Cruciani, G. (1999) Crystal-chemistry and synchrotron Rietveld refinement of two different clinoptilolites from volcanoclastites of North-Western Sardinia. European Journal of Mineralogy, 11, 1051–1060.

Casey, W.H., Westrich, H.R., and Arnold, G.W. (1988) Surface chemistry of labradorite feldspar reacted with aqueous solutions at pH = 2, 3 and 12. Geochimica et Cosmochimica Acta, 52, 2795–2807.

Cerri, G., Langella, A., Pansini, M., and Cappelletti, P. (2002) Methods of determining cation exchange capacities for clinoptilolite-rich rocks of the Logudoro region in northern Sardinia, Italy. Clays and Clay Minerals, 50, 127–135.

Chelishchev, N.F., Berenshtein, B.G., Berenshtein, T.A., Gribanova, N.K., and Martynova, N.S. (1973) Ion-exchange properties of clinoptilolites. Doklady Akademii Nauk, 210, 1110–1112.

Colella, C. (1996) Ion exchange equilibria in zeolite minerals. Mineralium Deposita, 31, 554–562.

Coombs, D., Alberti, A., Armbruster, T., Artioli, G., Collela, C., Galli, E., Grice, J., Liebau, F., Mandarino, J., Minato, H., Nickel, E., Passglia, E., Peacor, D., Quartieri, S., Rinaldi, R., Ross, M., Sheppard, R., Tillmanns, E., and Vezzalini, G. (1998) Recommended nomenclature for zeolite minerals; report of the Subcommittee on Zeolites of the International Mineralogical Association, Commission on New Minerals and Mineral Names. Mineralogical Magazine, 62, 533–571.

Daniels, E.A. and Puri, M. (1986) Physico-Chemical investigations of gamma-ir-

radiated zeolite-4A. Radiation Physics and Chemistry, 27, 225–227.
Debye, P. and Hückel, E. (1923) On the theory of electrolytes. Zeitschrift für Physik, 24, 185–208.
Dyer, A., Enamy, H., and Townsend, R.P. (1981) The plotting and interpretation of ion exchange isotherms in zeolites. Separation Science and Technology, 16, 173–183.
Elizondo, N.V., Ballesteros, E., and Kharisov, B.I. (2000) Cleaning of liquid radioactive wastes using natural zeolites. Applied Radiation and Isotopes, 52, 27–30.
Ermatov, S.E., Mosienko, T.A., and Orozbaev, R. (1980) The surface interaction and structure of an irradiated zeolite. Russian Journal of Physical Chemistry, 54, 1436–1438.
Faghihian, H., Ghannadi Marageh, M., and Kazemian, H. (1999) The use of clinoptilolite and its sodium form for removal of radioactive cesium and strontium from nuclear wastewater and Pb^{2+}, Ni^{2+}, Cd^{2+}, Ba^{2+} from municipal wastewater. Applied Radiation and Isotopes, 50, 655–660.
Finger, L.W. (1989) Synchrotron powder diffraction. In D.L. Bish and J.E. Post, Eds., Modern powder diffraction, 20, p. 309–331. Reviews in Mineralogy, Mineralogical Society of America, Chantilly, Virginia.
Fletcher, P. and Townsend, R.P. (1981) Transition metal ion exchange in zeolites. Journal of the Chemical Society Faraday Transactions 1, 77, 497–509.
Franklin, K.R. and Townsend, R.P. (1985a) Multicomponent ion exchange in zeolites. Journal of the Chemical Society Faraday Transactions 1, 81, 1071–1086.
——— (1985b) Multicomponent ion exchange in zeolites. Journal of the Chemical Society Faraday Transactions 1, 81, 3127–3141.
Fullerton, R. (1961) The effect of gamma radiation on clinoptilolite U.S. Atomic Energy Commission, Doc. No. HW-69256.
Gaines, L.G. and Thomas, H.C. (1953) Adsorption studies on clay minerals. II. Formulation of the thermodynamics of exchange adsorption. Journal of Chemical Physics, 21, 714–718.
Glueckauf, E. (1949) Activity coefficients in concentrated solutions containing several electrolytes. Nature, 163, 414–415.
Gottardi, G. (1989) The genesis of zeolites. European Journal of Mineralogy, 1, 479–487.
Gottardi, G. and Galli, E. (1985) Natural zeolites. Springer-Verlag, New York.
Gournis, D., Mantaka-Marketou, A.E., Karakassides, M.A., and Petridis, D. (2001) Ionizing radiation-induced defects in smectite clays. Physics and Chemistry of Minerals, 28, 285–290.
Gu, B.X., Wang, L.M., and Ewing, R.C. (2000) The effect of amorphization on the Cs ion exchange and retention capacity of zeolite-NaY. Journal of Nuclear Materials, 278, 64–72.
Güntelberg, E. (1926) Interaction of ions. Zeitschrift für Physikalische Chemie, 123, 199–247.
Hay, R.L. (1977) Geology of Zeolites in Sedimentary Rocks. In F.A. Mumpton, Ed., Mineralogy and geology of natural zeolites, 4, p. 53–64. Reviews in Mineralogy (formerly known as Short Course Notes), Mineralogical Society of America, Chantilly, Virginia.
Hay, R.L. and Sheppard, R.A. (2001) Occurrence of zeolites in sedimentary rocks: An overview. In D.L. Bish and D.W. Ming, Eds., Natural zeolites: Properties applications and uses, 45, p. 217–232. Reviews in Mineralogy and Geochemistry, Mineralogical Society of America, Chantilly, Virginia.
Hill, R.J. and Howard, C.J. (1987) Quantitative phase analysis from neutron powder diffraction data using the rietveld method. Journal of Applied Crystallography, 20, 467–474.
Inglezakis, V.J. (2005) The concept of "capacity" in zeolite ion-exchange systems. Journal of Colloid and Interface Science, 281, 68–79.
Inglezakis, V., Diamandis, A., Loizidou, M., and Grigoropoulou, H. (1999) Effect of pore clogging on Kinetics of lead uptake by clinoptilolite. Journal of Colloid and Interface Science, 215, 54–57.
Inglezakis, V.J., Loizidou, M.D., and Grigoropoulou, H.P. (2003) Ion exchange of Pb^{2+}, Cu^{2+}, Fe^{3+}, and Cr^{3+} on natural clinoptilolite selectivity determination and influence of acidity on metal uptake. Journal of Colloid and Interface Science, 261, 49–54.
——— (2004) Ion exchange studies on natural and modified zeolites and the concept of exchange site accessibility. Journal of Colloid and Interface Science, 275, 570–576.
Jama, M.A. and Yücel, H. (1990) Equilibrium studies of sodium-ammonium, potassium-ammonium and calcium-ammonium exchanges on clinoptilolite zeolite. Separation Science and Technology, 24, 1393–1416.
Jastrezbski, Z. (1987) The nature and properties of engineering materials. Wiley, New York.
Kielland, J. (1935) Thermodynamics of base-exchange equilibria of some different kinds of clays. Journal of the Society of Chemical Industry, 54, 232–234.
Komarneni, S., Plau, G.L., and Pillay, K.K.S. (1983) Radiation effects on a zeolite ion exchange and a pollucite. Nuclear and Chemical Waste Management, 4, 335–338.
Koyama, K. and Takeuchi, Y. (1977) Clinoptilolite: the distribution of potassium atoms and its role in thermal stability. Zeitschrift fur Kristallograhie, 145, 216–239.
Langela, A., Pansini, M., Cappelletti, P., Gennaro, B., Gennaro, M., and Colella, C. (2000) NH_4^+, Cu^{2+}, Zn^{2+}, Cd^{2+} and Pb^{2+}, exchange for Na^+ in a sedimentary clinoptilolite, North Sardinia, Italy. Microporous Mesoporous Material, 37, 337–343.
Lehto, J. and Harjula, R. (1995) Experimentation in ion exchange studies—the problem of getting reliable and comparable results. Reactive Functional Polymers, 27, 121–146.
Liu, X. and Thomas, K.J. (1995) Time-resolved diffuse reflectance of electron trapping by alkali-metal cation clusters in zeolites and clays following Far-UV excitation. Journal of the Chemical Society Faraday Transactions, 91, 759–765.
Liu, X., Zhang, G., and Thomas, K.J. (1995) Spectroscopic studies of electron trapping in zeolites: Cation cluster trapped electrons and hydrated electrons. Journal of Physical Chemistry, 99, 10024–10034.
Loizidou, M. (1982) Ion exchange of lead and cadmium with the sodium and ammonium forms of some natural zeolites. Ph.D. thesis, City University, London.
Loizidou, M. and Townsend, R.P. (1987) Ion exchange properties of natural clinoptilolite, ferrienite and mordenite: Part 2. Lead-sodium and lead-ammonium equilibria. Zeolites, 7, 153–159.
Marinin, D.V. and Brown, G.N. (2000) Studies of sorbent/ion-exchange materials for the removal of radioactive strodium from liquid radioactive waste and high hardness groundwaters. Waste Management, 20, 545–553.
Meier, W.M. and Olson, D.H. (1992) Atlas of zeolite structure types. Zeolites, 12, 1–200.
Melamed, R. and Benvido, da Luz Adao (2006) Efficiency of industrial minerals on the removal of mercury species from liquid effluents. Science of the Total Environment, 368, 403–406.
Mercer, B.W. and Ames, L.L. (1978) Zeolite ion exchange in radioactive and municipal wastewater treatment. In L.B. Sands and F.A. Mumpton, Eds., Natural zeolites: Occurrence, properties use, p. 451–461. Pergamon Press, Oxford.
Ming, D.W. and Boettinger, J.L. (2001) Zeolites in Soil Environments: An overview. In D.L. Bish and D.W. Ming, Eds., Natural zeolites: Properties applications and uses, 45, p. 323–345. Reviews in Mineralogy and Geochemistry, Mineralogical Society of America, Chantilly, Virginia.
Ming, D.W. and Dixon, J.B. (1986) Clinoptilolite in south Texas soils. Soil Science Society of America Journal, 50, 1618–1622.
Misaelides, P., Godelitsas, A., and Filippidis, A. (1995a) The use of zeoliferous rocks from Metaxades-Thrace, Greece, for the removal of caesium from aqueous solutions. Fresenius Environment bulletin, 4, 227–231.
Misaelides, P., Godelitsas, A., Filippidis, A., Charistos, D., and Anousis, I. (1995b) Thorium and uranium uptake by natural zeolitic materials. Science of the Total Environment, 173/174, 237–246.
Nilchi, A., Khanchi, A., Ghanadi, M.M., and Bagheri, A. (2003) Investigation of the resistance of some naturally occurring and synthetic inorganic ion exchangers against gamma radiation. Radiation Physics and Chemistry, 66, 167–177.
Nordstrom, D.K. and Munoz, J.L. (1994) Geochemical Thermodynamics, 2nd ed. Blackwell Scientific Publications, Boston.
Pabalan, R.T. (1994) Thermodynamics of ion exchange between clinoptilolite and aqueous solutions of Na^+/K^+ and Na^+/Ca^+. Geochimica et Cosmochimica Acta, 58, 4573–4590.
Pabalan, R.T. and Bertetti, F.P. (1994) Thermodynamics of ion exchange between Na^+/Sr^{2+} solutions and the zeolite mineral clinoptilolite. Materials Research Society Symposium, Proceedings, 333, 731–738.
Passaglia, E. and Sheppard, R.A. (2001) The crystal chemistry of zeolites: An overview. In D.L. Bish and D.W. Ming, Eds., Natural zeolites: Properties applications and uses, 45, p. 69–116 Reviews in Mineralogy and Geochemistry, Mineralogical Society of America, Chantilly, Virginia.
Petrosov, I.Kh. and Jarbashian, R.T. (1999) Main Zeolite Deposits of Armenia. Armenian Academy Edition, Yerevan (in Russian).
Petrosov, I.Kh. and Sadoyan, A.A. (1998) New Zeolite deposits spread in Armenia. Proceedings of Armenian National Academy, Earth Sciences, II, 3, 39 (in Russian).
Petrov, O.E., Filizova, L.D., and Kirov, G.N. (1991) Cation distribution in clinoptilolite structure: Cs-exchanged sample. Comptes Rendus de l' Académie Bulgare des Sciences, 44, 77–80.
Petrus, R. and Warchol, J.K. (2005) Heavy metal removal by clinoptilolite. An equilibrium study in multi-component systems. Water Research, 39, 819–830.
Pillay, K.K.S. and Palau, G.L. (1982) Radiolytic effects on ion exchangers during storage of radioactive waste. Proceedings of the International Conference on Radioactive Waste Management, 204–210.
Pitzer, K.S. (1991) Ion interaction approach: Theory and data correlation. In K.S. Pitzer, Ed., Activity coefficients in electrolyte solutions, 2nd ed., p. 75–153. University of California, Berkley.
Ragnarsdóttir, K.V., Graham, C.M., and Allen, G.C. (1996) Surface chemistry of reacted heulandite determined by SIMS and XPS. Chemical Geology, 131, 167–181.
Rees, L.V.C. (1980) Binary and ternary ion exchange in zeolite A. In R.P. Townsend, Ed., The properties and applications of zeolites, 33, p. 218–243. The Chemical Society, London.
Robinson, R.A. and Stokes, R.H. (1970) Electrolyte solutions, 2nd ed. Butterworths, London.

Sherry, H. (1966) The ion exchange properties of zeolites, I, Univalent ions. Journal Physical Chemistry, 70, 1158–1168.

Smyth, J.R. (1982) Zeolite stability constraints on radioactive waste isolation in zeolite-bearing volcanic rocks. Journal of Geology, 90, 195–202.

Smyth, J.R., Spaid A.T., and Bish, D.L. (1990) Crystal structures of a natural and a Cs-exchange clinoptilolite. American Mineralogist, 75, 522–528.

Spinks, J.W.T. and Woods, R.J. (1990) An Introduction to radiation chemistry, 3rd ed. John Wiley and Sons Inc., New York.

Valcke, E., Engels, B., and Cremers, A. (1997a) The use of zeolites as amendments in radiocaesium- and radiostrontium-contaminated soils: A soil-chemical approach. Part I: Cs-K exchange in clinoptilolite and mordenite. Zeolites, 18, 205–211.

——— (1997b) The use of zeolites as amendments in radiocaesium and radiostrontium contaminated soils: A soil chemical approach. Part II: Sr-Ca exchange in clinoptilolite and mordenite and Zeolite A. Zeolites, 18, 212–217.

Vaniman, D.T., Chipera, S.J., Bish, D.L., Carey, J.W., and Levy, S.S. (2001) Quantification of unsaturated-zone alteration and cation exchange in zeolitized tuffs at Yucca Mountain, Nevada, U.S.A. Geochimica et Cosmochimica Acta, 65, 3409–3433.

Vlessidis, A.G., Triantafillidis, C.S., and Evmeridis, N.P. (2001) Removal and recovery of p-phenylenediamines developing compounds from photofinishing lab-washwater using clinoptilolite tuffs from Greece. Water Research, 35, 1603–1608.

Wang, S.X., Wang, L.M., and Ewing, R.C. (2000) Electron and ion irradiation of zeolites. Journal of Nuclear Materials, 278, 233–241.

Yamamoto, S., Sugiyama, S., Matsuoka, O., Kohmura, K., Honda, T., Banno, Y., and Nozoye, H. (1996) Dissolution of zeolite in acidic aqueous solutions as revealed by AFM imaging. Journal of Physical Chemistry, 100, 18474–18482.

Yang, P. and Armbruster, T. (1996) Na, K, Rb, and Cs Exchange in Heulandite Single-Crystals: X-ray Structure Refinements at 100 K. Journal of Solid State Chemistry, 123, 140–149.

Zamzow, M.J., Eichbaum, B.R., Sandgren, K.R., and Shanks, D.E. (1990) Removal of heavy metals and other cations from wastewater using zeolites. Separation Science and Technology, 25, 1555–1569.

Zhang, G., Liu, X., and Thomas, K. (1998) Radiation induced physical and chemical processes in zeolite materials. Radiation Physics and Chemistry, 51, 135–152.

Manuscript received December 22, 2006
Manuscript accepted June 6, 2007
Manuscript handled by Richard Wilkin